Response to reviewer #1's comments

Reviewer comments are in **bold**. Author responses are in plain text. Excerpts from the manuscript are in *italics*. Modifications to the manuscript are in *blue italics*. Page and line numbers in the responses correspond to those in the original AMTD paper.

The authors are describing experimental findings from an online method for the detection of thermalized Criegee intermediates (CI) and RO_2 radicals in different laboratory setups. CIs have been observed via HFA titration or DMPO derivatization and RO_2 radicals via DMPO or TEMPO derivatization. Analysis was carried out by means of a PTR3 mass spectrometer running in the H_3O^+ or NH_4^+ mode. CI detection via HFA adducts was successful in the case of the ozonolysis of TME, isoprene, pentene and hexene, but not for the expected CIs arising from the ozonolysis of selected terpenes. Also the simplest CI, CH_2OO, was not measurable. Examples for RO_2 measurements are given from the ozonolysis (incl. OH reaction?) of TME and alpha-pinene. The stated detection limit for CIs is about 10^7 molecules/cc and that for RO_2 about 10^8 molecules/cc for 30 s integration time. The topic of this paper is well suited for AMT. Some clarifications are needed before publication can be recommended.

We would like to thank the reviewer for the positive reception of our work and constructive comments that helped us to improve our manuscript. Below we provide our replies to the reviewer's comments. Page and line numbers in the responses correspond to those in the AMTD paper.

1. **Line 53: Atmospheric RO_2 radical concentrations in the order of 10^8 molecules/cc are not generally valid. It stands mainly for CH_3O_2, concentration levels of other RO_2 radicals can be much lower.**

   We modify the following sentence by specifying ambient concentrations of RO_2 species (P2 L52):

   Highly sensitive detection systems are required to determine the minute concentrations of these species, ~~which are typically on the order of 10^8 molecule cm^{-3} for organic peroxy radicals (Fuchs et al., 2008) and are expected to be less than 10^5 molecule cm^{-3} for SCIs (Novelli et al., 2017)~~. Concentrations of the smallest organic peroxy radicals, CH_3O_2, are typically on the order of 10^8 molecule cm^{-3} while concentrations of other RO_2 species can be much lower (Fuchs et al., 2008). As for SCIs, their concentrations are expected to be less than 10^5 molecule cm^{-3} (Novelli et al., 2017).

2. **Line 104: Please provide a table with the initial reactant concentrations and the calculated amount of reacted olefin for a better understanding what has been done.**

   We include the following table containing the initial reactant concentrations and the calculated amount of reacted olefin in the SI:

   Table S2: Descriptions of ozonolysis experiments with HFA

Olefin	*Initial olefin concentration, molecule cm^{-3}*	*O_3 concentration, molecule cm^{-3}*	*HFA concentration, molecule cm^{-3}*	*Calculated amount of reacted olefin, %*

TME	$1.85 \cdot 10^{12}$	$1.67 \cdot 10^{13}$	$6.09 \cdot 10^{15}$	17%
isoprene	$1.23 \cdot 10^{13}$	$3.20 \cdot 10^{14}$	$5.35 \cdot 10^{15}$	6%
pentene	$4.18 \cdot 10^{13}$	$6.15 \cdot 10^{13}$	$5.35 \cdot 10^{15}$	14%
hexene	$2.21 \cdot 10^{13}$	$2.95 \cdot 10^{14}$	$5.35 \cdot 10^{15}$	50%
α-pinene	$2.70 \cdot 10^{12}$	$3.20 \cdot 10^{14}$	$5.35 \cdot 10^{15}$	37%
limonene	$2.10 \cdot 10^{12}$	$3.45 \cdot 10^{14}$	$5.35 \cdot 10^{15}$	67%

3. Line 143: Also here, please state the initial reactant conditions. What was the residence time in the respective flow tubes? If I understand it right, in the first flow tube the O_3(OH?) + TME/alpha-pinene reaction was running without OH scavenger and the second flow tube served for product derivatization by DMPO (but TME/alpha-pinene conversion was still running)? Please provide a more precise insight what's going on in the different parts of this flow-through experiment.

We add the following discussion on the experimental setup used during the ozonolysis experiments with spin trap DMPO (P5 L146):

Experimental setup consisted of two identical ~2.1L flow reactors. The parent hydrocarbon was mixed with ozone in the first flow ~~tube~~ reactor with a residence time of ~28s. Similar to the previous ozonolysis experiments described in Sect. 2.1, the parent olefin was vaporized from a flask filled with pure substance by passing zero air regulated by a mass flow controller, and ozone was generated using a low-pressure mercury ultraviolet lamp. ~~while the spin trap DMPO ($C_6H_{11}NO$) was introduced in the second flow tube using an LCU.~~ We used an LCU to introduce the spin trap DMPO in the second flow reactor with a residence time of ~23s. A known amount (up to 10 μL min^{-1}) of the DMPO solution was evaporated into a humidified gas stream of synthetic air (5.4-7 SLPM), resulting in the gas-phase DMPO concentration of up to 1.1×10^{13} molecule cm^{-3}. The second flow reactor served for derivatization of SCIs and RO_2 species by DMPO while the parent hydrocarbon was still reacting with ozone. Hence, we conducted integrated production measurements of SCIs and RO_2 species formed in both flow reactors. The PTR3 was used to detect ~~spin trap adducts with SCIs and RO2 species~~ SCI·DMPO and RO_2·DMPO adducts, while ozone levels were observed using an ozone monitor (2B Technologies).

In addition, we include the following table containing the initial reactant concentrations and the calculated amount of reacted olefin in the SI:

Table S3: Descriptions of ozonolysis experiments with DMPO

Olefin	*Initial olefin concentration, molecule cm^{-3}*	*O_3 concentration, molecule cm^{-3}*	*DMPO concentration, molecule cm^{-3}*	*Calculated amount of reacted olefin, %*
TME	$3.69 \cdot 10^{11}$	$7.87 \cdot 10^{12}$	$2.01 \cdot 10^{12}$	43%
α-pinene	$4.92 \cdot 10^{11}$	$1.03 \cdot 10^{13}$	$1.10 \cdot 10^{13}$	9%

4. **Line 186: The Donahue group, ref: 10.1021/jp108773d, used $\mathbf{k_{(CH_3)_2COO+HFA} = 2 \times 10^{-13}}$ cc/s, about 2 orders of magnitude lower as the rate coefficient used in this work. Is the HFA concentration still high enough for complete conversion of $(CH_3)_2COO$ with HFA?**

   Since the proton affinity of HFA is lower than that of water, we were able to introduce significant amounts of HFA (see Table S2 above) to make sure that HFA remains the major chemical loss even if $k_{(CH_3)_2COO+HFA} = 2 \times 10^{-13}$ molecule cm^{-3} s^{-1}. We update Fig S3 in the SI:

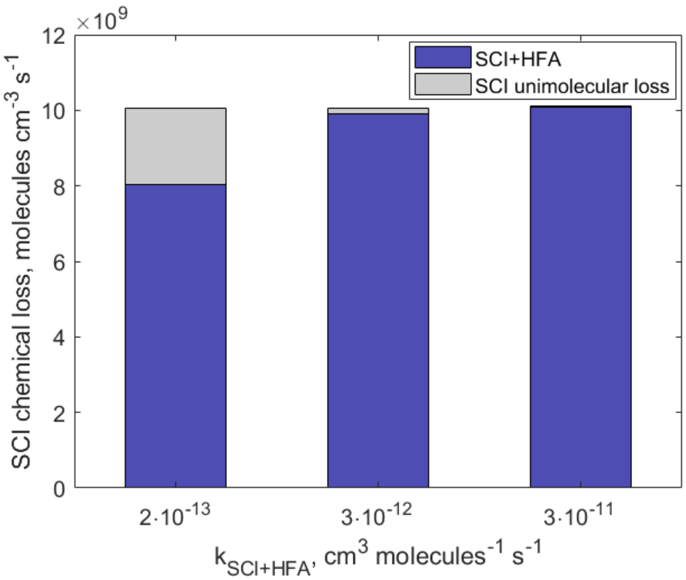

   Figure S3: Chemical losses of stabilized Criegee intermediates (CH3)2COO calculated assuming different $k_{SCI+HFA}$ reaction rates under experimental conditions. $k_{SCI+HFA} = 3 \times 10^{-11}$ cm^3 molecule^{-1} s^{-1} corresponds to the rate constant for CH_2OO + HFA reaction (Taatjes et al., 2012). Previous studies used lower rate constant (2×10^{-13} molecule cm^{-3} s^{-1}; Drozd et al., 2011). Even at lower values of the reaction rate the major chemical loss pathway for SCI is the reaction with HFA.

   We also add the reference to the work by the Donahue group in the manuscript (P6 L187):

   It has been suggested that the reaction between HFA and acetone oxide may be slower compared to the CH_2OO one (Murray et al., 1965; Taatjes et al., 2012) while $k_{(CH_3)_2COO+HFA} = 2 \times 10^{-13}$ molecule cm^{-3} s^{-1} was used in the previous studies (Drozd et al., 2011).

5. **Line 197: How good is the agreement model vs. measurement in the case of the ozonolysis of isoprene, pentene and hexene?**

   In the case of the ozonolysis of isoprene, pentene and hexene, our measurements of SCI·HFA are one to two orders of magnitude lower than the model prediction. There are several factors that can contribute to this discrepancy:

   1. Yields of SCIs for larger intermediates might be off. MCM assumes the same yield of 0.18 for CH_3CHOO, CH_3CH_2CHOO and $CH_3CH_2CH_2CHOO$, however, measured yields of these intermediates vary by up to a factor of 2 (Newland et al., 2015 and references therein). In

addition, some studies suggested that yields of larger SCIs (e.g., C_4-SCI) are significantly smaller than that of CH_2OO (Nguyen et al., 2016).

2. Unimolecular decomposition of SCI is not taken into account in the model. MCM includes only bimolecular loss reactions for CH_3CHOO, CH_3CH_2CHOO and $CH_3CH_2CH_2CHOO$, while some studies suggest that SCI unimolecular rates increase with size and become more important (Nguyen et al., 2016; Newland et al., 2015).
3. The reaction rate coefficient between larger SCI and the derivatization agent HFA is unknown. As the reviewer pointed out earlier, the reaction rate coefficient is expected to be lower for larger SCIs, but it has not been measured directly. While we introduced significant amounts of HFA in the experimental system to ensure that the reaction with HFA remains the major chemical loss for SCIs, we cannot be certain that all SCIs were scavenged by HFA.

Based on these factors and associated uncertainties in both the model and measurements, we think that presenting the model vs. measurement agreement for isoprene, pentene, and hexene falls beyond the scope of this study.

6. **Line 204: What is the detection limit of OH radicals via the TEMPO derivatization as a result of this work? Giorio et al., ref:10.1021/jacs.6b10981, were not able to follow OH production from alpha-pinene ozonolysis using a similar technique. Is it really possible to measure steady-state OH in a reaction system by means of this technique?**

We estimate the detection limit of OH radicals via the TEMPO derivatization for our setup to be ~6×10^6 molecule cm^{-3}. This limit of detection is calculated for a 1 s integration time of TEMPO·OH signal as three standard deviations of measured background divided by derived sensitivity for TEMPO. The purpose of TEMPO derivatization experiments was to demonstrate that chemical derivatization agents, including spin traps, are highly reactive towards atmospheric radicals and reactive intermediates rather than to fully describe this method to detect OH radicals. As we state in the manuscript (P7 L219), further tests are required to compare the measurement capability of this method with that of a well-established technique, such as LIF. Whether steady-state OH concentration can be measured will depend on the experimental setup and what averaging time is acceptable. For example, with 10 min averaging the detection limit can be reduced to 2.5×10^5 molecule cm^{-3}, which is in a useful range. Furthermore, other CIMS instruments have achieved lower detection limits. Thus, we believe detection of OH is feasible, depending on conditions and instrumentation. While we agree with the reviewer that it would be interesting to check if it would be possible to observe OH from α-pinene ozonolysis, we think that conducting such experiments lies beyond the scope of this manuscript.

7. **Line 222: I think these experiments have been done in the double flow-tube setup, right? So, you should see the resulting RO_2 radicals from ozonolysis as well as those from the OH reaction if no OH scavenger is used. That means in the case of TME also the primarily formed HO-$C_6H_{12}O_2$ radicals should be visible in addition to acetonylperoxy radicals from the ozone reaction? And in the case of alpha-pinene, HO-$C_{10}H_{16}O_2$ radicals (and subsequent autoxidation products) must be there along with the ozonolyis-derived RO_2s. Please comment!**

We observed formation of RO_2 species formed via OH-oxidation of TME. We include the following discussion (P8 L239) and edit Fig. 6 by adding the corresponding tracer to it:

OH radicals, formed via decomposition of SCI, can in turn react with TME and lead to formation of another RO_2 species $OH\text{-}C_6H_{12}OO\cdot$. This radical was detected as the $C_6H_{13}O_3\cdot$DMPO adduct ($C_{12}H_{24}NO_4$, m/z 264.205; Fig. 6).

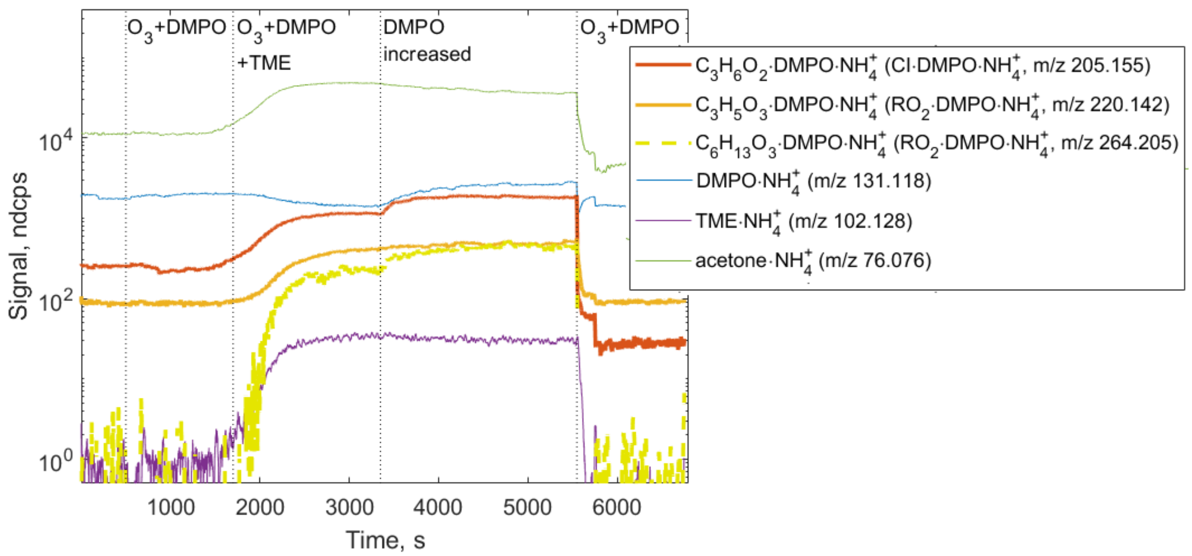

Figure 6: Ion tracers observed by NH_4^+ CIMS in a TME ozonolysis experiment as a function of different reactant conditions. Reactant concentrations are [TME] = 3.69×10^{11}; [O_3] = 7.87×10^{12}; [DMPO] = 2.01×10^{12} molecule cm^{-3}.

In addition, we also observed formation of $HO\text{-}C_{10}H_{16}O_2$ species and subsequent autooxidation products in the case of α-pinene. We include the following discussion (P9 L261) and edit Figs. S10 and S11:

OH radicals, formed via decomposition of SCI, can in turn react with α-pinene and lead to formation of OH-derived RO_2 species $C_{10}H_{17}O_3$ and subsequent autoxidation RO_2 species $C_{10}H_{17}O_5$ (Berndt et al., 2016). These radicals were detected as the $RO_2\cdot$DMPO adducts (Figs. S10 and S11).

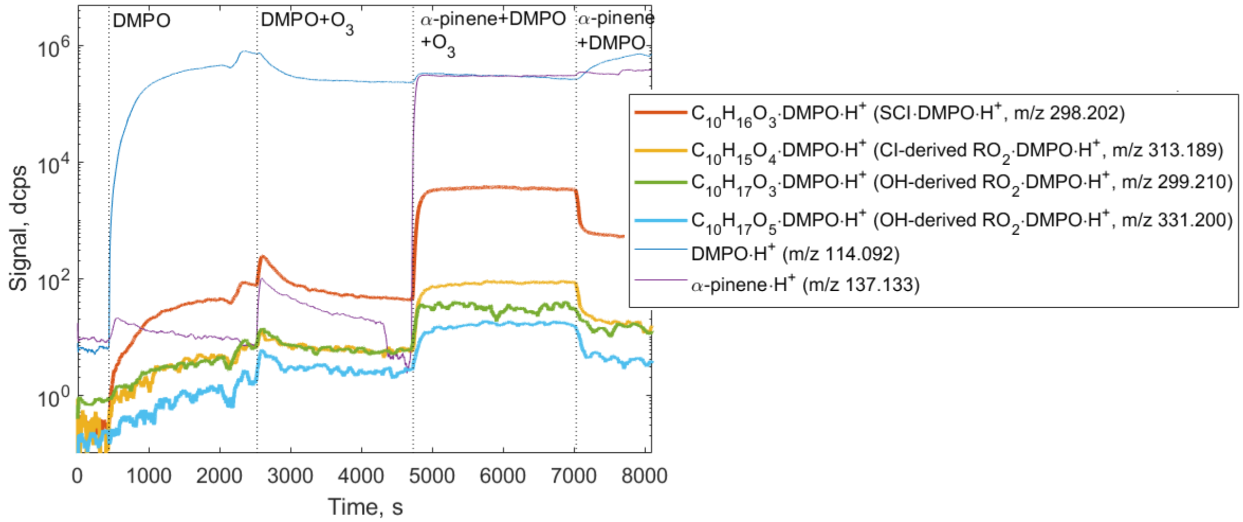

Figure S10: Ion tracers observed by H_3O^+ CIMS in an α-pinene ozonolysis experiment as a function of different reactant conditions. Reactant concentrations are [α-pinene] = 4.92×10^{11}; [O_3] = 1.03×10^{13}; [DMPO] = 1.10×10^{13} molecule cm^{-3}.

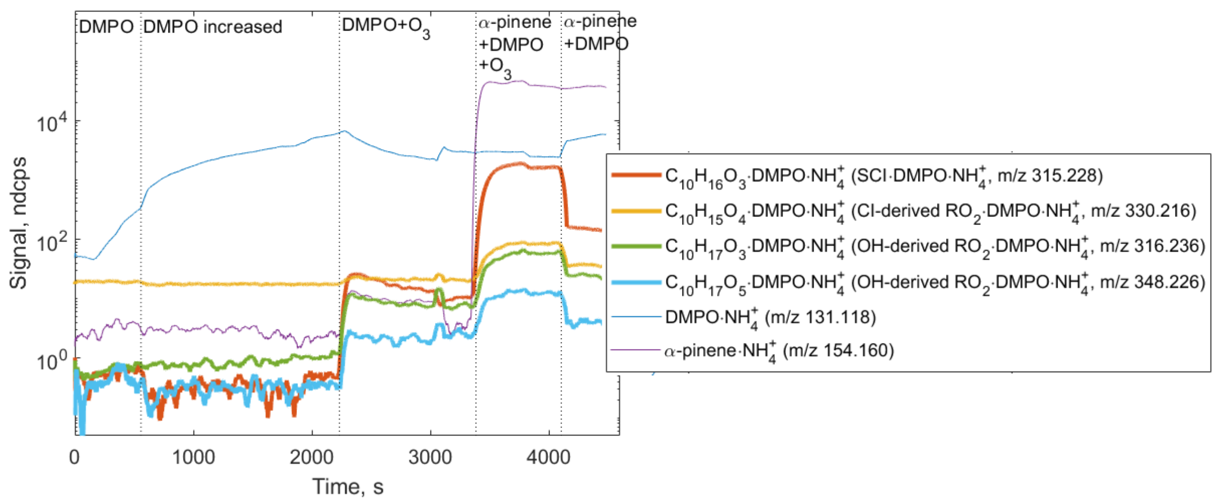

Figure S11: Ion tracers observed by NH_4^+ CIMS in an α-pinene ozonolysis experiment as a function of different reactant conditions. Reactant concentrations are [α-pinene] = 4.92×10^{11}; [O_3] = 1.03×10^{13}; [DMPO] = 1.10×10^{13} molecule cm^{-3}.

8. **Another point: Hansel et al., ref: 10.1016/j.atmosenv.2018.04.023, are stating a detection limit of 2×10^5 molecules/cc for RO_2 radicals and closed shell products from cyclohexene ozonolysis using a similar (or same) mass spec with NH_4^+ ionization. That means the authors should be able to monitor the RO_2 radicals directly at the outflow w/o derivatization? That could be helpful for the assessment of the derivatization procedure.**

We agree with the reviewer that it would be interesting to conduct simultaneous measurements of RO_2 species with and without using derivatization agents, however, our setup was not designed for this type of experiments. In addition, there are several disadvantages associated with direct measurements of RO_2 species: (1) potential interferences from secondary chemistry, i.e., additional sources or radical production and destruction as well as their cycling, have to be taken into account; (2) losses of radicals on the walls in the experimental setup and inside the instrument have to be considered; and (3) potential interferences with isotopes of closed-shell molecules can impede quantification of detected RO_2 species. For example, an isotope of pinonic acid (*m/z* 203.148 in NH_4^+ CIMS) strongly overlaps with OH-derived RO_2 species formed via oxidation of α-pinene (*m/z* 203.152 in NH_4^+ CIMS).

9. **Line 259 and fig.8: Higher oxidized RO_2 radicals arising from pure autoxidation steps show a mass difference of 32 mass units due to step-by-step insertion of molecular oxygen. A mass difference of 16 mass units points to efficient bimolecular RO_2 steps altering the autoxidation-governed RO_2 distribution. So, as already said, it would be fine to have the complete reaction conditions to get an idea how important $RO_2 + RO_2$ could be.**

   The reviewer raises an interesting point. We agree that having a more complete understanding of the importance of RO_2 self-reactions could be beneficial for this study. However, to the best of our knowledge, kinetics of autoxidation and self-reactions is well studied for smaller RO_2 species only. Hence, we believe that determining the relative importance of chemical loss channels for RO_2 species lies beyond the scope of this study.

References:

Berndt, T., Richters, S., Jokinen, T., Hyttinen, N., Kurtén, T., Otkjær, R.V., Kjaergaard, H.G., Stratmann, F., Herrmann, H., Sipilä, M., Kulmala, M., and Ehn, M.: Hydroxyl radical-induced formation of highly oxidized organic compounds, Nature Communications, 7, 13677, DOI: 10.1038/ncomms13677, 2016.

Drozd, G.T., Kroll, J.H., and Donahue, N.M.: 2,3-Dimethyl-2-butene (TME) Ozonolysis: Pressure Dependence of Stabilized Criegee Intermediates and Evidence of Stabilized Vinyl Hydroperoxides, J. Phys. Chem. A 2011, 115, 161–166, DOI: 10.1021/jp108773d, 2011.

Newland, M.J., Rickard, A.R., Alam, M.S., Vereecken, L., Munoz, A., Rodenasd, M. and Bloss, W.J.: Kinetics of stabilised Criegee intermediates derived from alkene ozonolysis: reactions with SO_2, H_2O and decomposition under boundary layer conditions. Phys. Chem. Chem. Phys., 17, 4076-4088, DOI: 10.1039/C4CP04186K, 2015.

Nguyen, T.B., Tyndall, G.S., Crounse, J.D., Teng, A.P., Bates, K.H., Schwantes, R.H., Coggon, M.M., Zhang, L., Feiner, P., Milller, D.O., Skog, K.M., Rivera-Rios, J.C., Dorris, M., Olson, K.F., Koss, A.R., Wild, R.J., Brown, S.S., Goldstein, A.H., de Gouw, J.A., Brune, W.H., Keutsch, F.N., Seinfeld, J.H., and Wennberg, P.O.: Atmospheric fates of Criegee intermediates in the ozonolysis of isoprene. Phys. Chem. Chem. Phys., 18, 10241-10254, DOI: 10.1039/C6CP00053C, 2016.

Response to reviewer #2's comments

Reviewer comments are in **bold**. Author responses are in plain text. Excerpts from the manuscript are in *italics*. Modifications to the manuscript are in *blue italics*. Page and line numbers in the responses correspond to those in the original AMTD paper.

This study presents the development of an online method for measurements of SCIs and RO_2 in laboratory experiments using chemical derivatization and spin trapping techniques combined with H_3O^+ and NH_4^+ chemical ionization mass spectrometry. Application of this method is demonstrated using laboratory ozonolysis experiments of multiple hydrocarbons including TME, isoprene, pentene, hexene, alpha-pinene and limonene. The detection limits of spin trap and chemical derivatization agent adducts are estimated to be $1.4{\cdot}10^7$ molecule cm^{-3} for SCIs and $1.6{\cdot}10^8$ molecule cm^{-3} for RO_2 for 30 s integration time for the instrumentation used in this study. This manuscript is well written and within the scope of the journal. I recommend this manuscript to be published in AMT after the following issues be addressed.

We would like to thank the reviewer for the positive reception of our work and constructive comments that helped us to improve our manuscript. Below we provide our replies to the reviewer's comments. Page and line numbers in the responses correspond to those in the AMTD paper.

1. **Page 6, Line 166-167: Is there any evidence for using HFA with SCIs to prevent secondary reactions?**

   HFA was used to study kinetics of various SCIs in the past (e.g., Drozd et al., 2011; Drozd and Donahue, 2011). In these studies, HFA was implemented to directly probe SCI formation.

   We modify the following paragraph by specifying that HFA was used to prevent SCI secondary reactions (P4 L109):

   SCIs are known to be highly reactive towards ketones, especially electron poor ones such as HFA (Horie et al., 1999; ~~Drozd et al., 2011; Drozd and Donahue, 2011;~~ Taatjes et al., 2012). HFA has been previously used to effectively scavenge SCIs and prevent their secondary chemistry to directly probe SCI formation (Drozd et al., 2011; Drozd and Donahue, 2011).

2. **Page 6, Line 191-194 and Page 8, Line 249-251: Could the author give more detailed explanations or quantitative analysis for these four reasons?**

   We add the following details to our description (P6 L191):

   This discrepancy can be explained by a combination of the following factors~~(:)~~. First, a fraction of $(CH_3)_2COO{\cdot}HFA$ adducts might be irreversibly deposited on the surfaces inside the experimental setup and the PTR 8000 instrument (Pagonis et al., 2017). ~~wall losses of $(CH_3)_2COO{\cdot}HFA$ in the experimental setup and the PTR 8000 instrument; (2)~~ In addition, the sensitivity of observed SCI·HFA adducts depends on the reaction rate constant of the adduct with H_3O^+ ion and the degree of fragmentation of protonated product ions $SCI{\cdot}HFA{\cdot}H^+$ (Yuan et al., 2017). Since the reaction rate constant of SCI·HFA with H_3O^+ ions is unknown, we assumed that all SCI·HFA adducts were *ionized via proton transfer from hydronium ions and therefore used the sensitivity we obtained from acetone calibration to quantify detected SCI·HFA species. In addition, we did not take into account possible fragmentation of SCI·HFA·H^+ ions which may impede their detection, although a first bond cleavage would likely only break the ozonide ring structure without loss of mass.* ~~*uncertainty in the sensitivity at which the SCI·HFA adducts were detected; (3) potential ion fragmentation of protonated SCI·HFA adducts; and (4)*~~ *Finally, uncertainty of the kinetic model output is determined by the uncertainty in the SCI yield, and unimolecular and bimolecular reaction rate coefficients* ~~*uncertainty in the SCI yield, and unimolecular and bimolecular reaction rate coefficients used in the kinetic model.*~~

We add the following details to our description (P8 L248):

Similar to experiments described in Sect. 3.1, several factors can contribute to this discrepancy: (1) gas-wall partitioning of RO_2 species and RO2·DMPO adducts in the experimental setup ~~*flow tube setup*~~ *and inside the PTR3 instrument; (2) uncertainty in sensitivity at which RO_2·DMPO adducts were detected; (3) potential fragmentation of RO_2·DMPO·NH_4^+ product ions; and (4) uncertainties in the reaction rate coefficient k_{RO_2+DMPO}.*

3. **Page 9, Line 277-278: Since there could be various RO_2 in ambient air, how does the author think about the feasibility of using the CID technique to measure ambient air?**

   The CID technique can be used to constrain the instrument sensitivity to compounds that cannot be calibrated directly, including dozens of oxygenated compounds that were produced during a photooxidation experiment in an environmental chamber (Zaytsev et al., 2019). While we plan to implement analytical techniques presented in this study for ambient measurements of atmospheric radicals in the future, we think that these experiments are out of the scope of the current work.

4. **Supplement page 8: In Figure S11, at the beginning of the period DMPO+O_3, why did the SCI adduct (m/z 315.228) get a little increasing?**

   There are two factors that could contribute to the increase of SCI·DMPO tracer (*m/z* 315.228) when DMPO and O_3 were present in the experimental setup:
   1. formation of an isomer with same molecular formula but potentially different structure
   2. change in humidity of sampled air which affects both primary ion signal and sensitivity to observed compounds. As one can notice, other tracers (e.g., $C_{16}H_{27}NO$·NH_4^+, *m/z* 154.160; $C_{16}H_{26}NO_5$·NH_4^+, *m/z* 330.216) also showed a little increase when ozone was introduced in the experimental setup.

5. **Page 8, Line 234 and Supplement page 2, Line7: The last two letters of the word "$CH_3C(=O)CH_2OO$" use two different fonts.**

   We thank the reviewer for spotting this typo and fix it in the revised manuscript.

References:

Pagonis, D., Krechmer, J. E., de Gouw, J., Jimenez, J. L., and Ziemann, P. J.: Effects of gas–wall partitioning in Teflon tubing and instrumentation on time-resolved measurements of gas-phase organic compounds, Atmos. Meas. Tech., 10, 4687–4696, DOI: 10.5194/amt-10-4687-2017, 2017.

Yuan, B., Koss, A.R., Warneke, C., Coggon, M., Sekimoto, K., and de Gouw, J.A.: Proton-Transfer-Reaction Mass Spectrometry: Applications in Atmospheric Sciences, Chem. Rev., 117, 13187–13229, DOI: 10.1021/acs.chemrev.7b00325, 2017.

Application of chemical derivatization techniques combined with chemical ionization mass spectrometry to detect stabilized Criegee intermediates and peroxy radicals in the gas phase

Alexander Zaytsev[1], Martin Breitenlechner[1], Anna Novelli[2], Hendrik Fuchs[2], Daniel A. Knopf[3], Jesse H. Kroll[4], and Frank N. Keutsch[1,5,6]

[1]John A. Paulson School of Engineering and Applied Sciences, Harvard University, Cambridge, MA 02138, USA
[2]Institute of Energy and Climate Research – Troposphere (IEK-8), Forschungszentrum Jülich GmbH, 52428 Jülich, Germany
[3]School of Marine and Atmospheric Sciences, Stony Brook University, Stony Brook, NY 11794, USA
[4]Department of Civil and Environmental Engineering, Massachusetts Institute of Technology, Cambridge, MA02139, USA
[5]Department of Chemistry and Chemical Biology, Harvard University, Cambridge, MA 02138, USA
[6]Department of Earth and Planetary Sciences, Harvard University, Cambridge, MA 02138, USA

Correspondence to: Alexander Zaytsev (zaytsev@g.harvard.edu) and Frank N. Keutsch (keutsch@seas.harvard.edu)

Abstract. Short-lived highly reactive atmospheric species, such as organic peroxy radicals (RO_2) and stabilized Criegee intermediates (SCIs), play an important role in controlling the oxidative removal and transformation of many natural and anthropogenic trace gases in the atmosphere. Direct speciated measurements of these components are extremely helpful for understanding their atmospheric fate and impact. We describe the development of an online method for measurements of SCIs and RO_2 in laboratory experiments using chemical derivatization and spin trapping techniques combined with H_3O^+ and NH_4^+ chemical ionization mass spectrometry (CIMS). Using chemical derivatization agents with low proton affinity, such as electron-poor carbonyls, we scavenge all SCIs produced from a wide range of alkenes without depleting CIMS reagent ions. Comparison between our measurements and results from numeric modelling, using a modified version of the Master Chemical Mechanism, shows that the method can be used for quantification of SCIs in laboratory experiments with detection limit of 1.4×10^7 molecule cm^{-3} for 30 s integration time with the instrumentation used in this study. We show that spin traps are highly reactive towards atmospheric radicals and form stable adducts with them by studying the gas-phase kinetics of their reaction with hydroxyl radical (OH). We also demonstrate that spin trap adducts with SCIs and RO_2 can be simultaneously probed and quantified under laboratory conditions with detection limit of 1.6×10^8 molecule cm^{-3} for 30 s integration time for RO_2 species with the instrumentation used in this study. Spin trapping prevents radical secondary reactions and cycling, which ensures that measurements are not biased by chemical interferences, and can be implemented for detecting RO_2 species in the ambient atmosphere.

1 Introduction

Earth's atmosphere is an oxidizing environment. The initial oxidation step of volatile organic compounds (VOCs) involves reaction of a parent hydrocarbon with an oxidant. The hydroxyl radical (OH) is the most important oxidant in the atmosphere, although oxidation can be also initiated by O_3, NO_3 and Cl- or Br-atoms. Generally, reaction of VOCs with OH, NO_3 and Cl-atoms occurs via H-abstraction or via addition to unsaturated carbon double bonds leading to the formation of alkyl radicals. This reaction is quickly followed by O_2 addition resulting in the production of organic peroxy radicals (RO_2). In an NO-rich environment, RO_2 radicals predominantly react with NO, while at lower NO concentrations reactions with the hydroperoxy radical (HO_2), potentially other RO_2, and unimolecular reactions become more important. The common tendency is the formation of closed-shell, more oxidized VOCs (OVOCs). OVOCs may have lower volatilities than the parent hydrocarbons and may partition to the particle phase, thereby contributing to secondary organic aerosol (SOA) formation. OH, HO_2 and RO_2 radicals can form a catalytic reaction cycle, which can lead to production of tropospheric ozone as a consequence of the shift in the NO/NO_2 ratio to favor formation of NO_2. This cycle is terminated by the formation of organic hydroperoxides and nitrates, which can be viewed as reservoirs of the corresponding radicals. Overall, atmospheric radicals, especially their cycling, play an important role in the formation of SOA and tropospheric ozone, as well as in controlling atmospheric oxidation capacity.

Organic peroxy radicals can also be formed via ozonolysis of unsaturated organic compounds. Ozonolysis of alkenes results in the formation of primary ozonides that promptly decompose to a stable carbonyl and a vibrationally excited carbonyl oxide, also known as a Criegee intermediate (CI), some of which are thermally stabilized (SCI). SCI primarily decompose or react with water vapor (Vereecken et al., 2017) but are also believed to play a role in oxidation of SO_2 to form H_2SO_4 in the tropical regions (Khan et al., 2018). *syn*-SCI can undergo a unimolecular reaction and form a vinyl hydroperoxide, which rapidly decomposes to an OH radical and a vinyl radical. This radical is in resonance with an acetonyl-type radical, which can combine with molecular oxygen to form an RO_2 species (Johnson and Marston, 2008).

Measurements of atmospheric radicals and reactive intermediates, such as RO_2 and SCIs, are challenging because of their high reactivity towards trace gases and surfaces and rapid cycling, which may lead to potential interferences. Highly sensitive detection systems are required to determine the minute concentrations of these species~~, which are typically on the order of 10^8 molecule cm^{-3} for organic peroxy radicals (Fuchs et al., 2008) and are expected to be less than 10^5 molecule cm^{-3} for SCIs (Novelli et al., 2017)~~. Concentrations of the smallest organic peroxy radicals, CH_3O_2, are typically on the order of 10^8 molecule cm^{-3} while concentrations of other RO_2 species can be much lower (Fuchs et al., 2008). As for SCIs, their concentrations are expected to be less than 10^5 molecule cm^{-3} (Novelli et al., 2017). With respect to RO_2 species, there are several field-deployable measurement techniques available for non-speciated measurements of the sum of RO_2. Matrix Isolation Electron Spin Resonance Spectroscopy (MIESR) is an established, but rarely used, method for field measurements (Mihelcic et al., 1985). MIESR is an offline technique with a low time resolution (~30 min), however, its main advantage is that it does not require instrument calibration. Besides MIESR, chemical amplification and conversion systems represent another class of instruments for field studies (Edwards et al., 2003; Hornbrook et al., 2011; Cantrell et al., 1984; Wood and Charest, 2014). In these systems peroxy radicals are not measured directly but are rather converted to other radicals or closed-shell molecules (e.g., NO_2 or H_2SO_4). A detection limit of 10^7 molecule cm^{-3} can be achieved at a temporal resolution of 15 s, however, discrimination of different RO_2 species is not possible (Edwards et al., 2003). In addition, secondary chemistry, i.e., additional sources of radical production and destruction, has to be considered, and care needs to be taken to ensure that measurements are not biased by any chemical interferences (Reiner et al., 1997). Finally, laser-induced fluorescence (LIF) was also applied for ambient measurements of RO_2 radicals (Fuchs et al., 2008). This technique is characterized by an excellent detection limit of $(2 - 7) \times 10^7$ molecule cm^{-3} for an integration time of 30 s. Similarly to chemical amplifier systems, LIF does not allow for differentiation of various RO_2 species, however, although it is indirect and converts RO_2 to OH it does not have an amplification chain. Recently, novel mass spectrometric techniques using different ionization schemes to directly detect individual RO_2 species were developed (Hansel et al., 2018; Berndt et al., 2018; Berndt et al., 2019; Nozière and Vereecken, 2019).

As for SCIs, indirect measurement techniques have been widely used. In these techniques SCIs are chemically converted to other species (e.g., H_2SO_4 or hydroxymethyl hydroperoxide, HMHP) (Berndt et al., 2014; Sipilä et al., 2014; Neeb et al., 1997). In 2008, the simplest SCI, CH_2OO, was directly detected for the first time (Taatjes et al., 2008). Later, synchrotron photoionization mass spectrometry was combined with the CI generation technique using diiodoalkane photolysis (Welz et al., 2012), which spurred several studies to examine kinetics of bimolecular and unimolecular SCI reactions (Taatjes et al., 2012; Lewis et al., 2015; Chhantyal-Pun et al., 2016). Recently two new techniques for direct measurements of SCIs using Fourier transform microwave spectroscopy and chemical ionization mass spectrometry (CIMS) were introduced (Womack et al., 2015; Berndt et al., 2017).

Despite the abundance of different analytical methods used for detection of atmospheric radicals and reactive intermediates, there is still a need for an online, direct, field-deployable technique for measuring these short-lived highly reactive compounds in a speciated way. Free radicals have been conventionally detected by chemical derivatization (CD) techniques including spin trapping in condensed-phase biological and chemical systems (Hawkins and Davies, 2014; Nosaka and Nosaka, 2017). Non-radical spin traps (e.g., nitrone spin traps) are known to react with free radicals to form stable radical adducts that can be detected with electron paramagnetic resonance spectroscopy (Roberts et al., 2016). In addition, radical spin traps (e.g., nitroxide radicals) are also highly reactive towards radical species such as C-centered radicals and form closed-shell adducts with them (Bagryanskaya and Marque, 2014). However, there are only few studies in which these techniques were applied for probing atmospheric radicals and intermediates. Watanabe et al. (1982) presented an offline method to quantify hydroxyl radicals using the spin trap α-4-pyridyl-*N*-*tert*-butylnitrone α-1-oxide (4-POBN) where condensed-phase stable adducts were detected by electron spin resonance. Recently, Giorio et al. (2017) used the spin trap 5,5-Dimethyl-1-pyrroline *N*-oxide (DMPO) to characterize SCIs by detecting gas-phase spin trap adducts with online mass spectrometry.

Here we explore three types of CD agents, including two spin trapping agents, and show how they can be used for detection and quantification of various atmospheric radicals and reactive intermediates (Fig. 1). First, we implement the CD agent hexafluoroacetone (HFA) to characterize a wide range of gas-phase SCIs. HFA is selectively reactive towards SCIs (i.e., it is unreactive towards OH, HO_2 and RO_2), forms stable secondary ozonides with them, and has high vapor pressure and low proton affinity (Fig. 1). Next, we use the radical spin trap (2,2,6,6-Tetramethylpiperidin-1-yl)oxyl (TEMPO) to demonstrate that spin traps are highly reactive towards radicals in the gas phase, by studying kinetics of TEMPO+OH reaction, and therefore can effectively scavenge atmospheric radicals. Finally, we utilize the non-radical spin trap DMPO to simultaneously detect atmospheric gas-phase radicals and intermediates, including SCIs and RO_2 species (Fig. 1). Spin trap adducts and secondary ozonides with CD agents are observed and quantified using H_3O^+ and NH_4^+ CIMS, which allows for speciated online measurements of stabilized Criegee intermediates and speciated RO_2 radicals formed via ozonolysis of a wide range of parent hydrocarbons. The analytical methods presented here can be used for quantification of speciated SCIs and RO_2 formed in laboratory experiments as well as for field measurements.

2 Methods

2.1 Ozonolysis experiments with chemical derivatization agent HFA

The ozonolysis experiments of multiple hydrocarbons including tetramethylethylene (TME), isoprene, pentene, hexene, α-pinene and limonene were conducted in a flow tube reactor at ambient pressure and temperature (~290 K) and dry conditions (relative humidity < 2%). The experimental setup consisted of a flow reactor system with a residence time of ~10 s. The parent hydrocarbon was mixed with ozone and the chemical derivatization agent HFA (C_3F_6O) in the flow reactor leading to the formation of SCIs and their scavenging as SCI·HFA adducts. SCIs are known to be highly reactive towards ketones, especially electron poor ones such as HFA (Horie et al., 1999; ~~Drozd et al., 2011; Drozd and Donahue,~~ 2011; Taatjes et al., 2012). HFA has been previously used to effectively scavenge SCIs and prevent their secondary chemistry to directly probe SCI formation (Drozd et al., 2011; Drozd and Donahue, 2011). The other advantage of employing this chemical derivatization agent is its relatively low proton affinity (PA 670.4 kJ/mol; Hunter and Lias, 1998). Since the PA of HFA is lower than that of water, HFA cannot be protonated in H_3O^+ CIMS. Hence, one can introduce significant amount of HFA to the system to make sure that all SCIs are scavenged very rapidly without any concern that H_3O^+ reagent ions would be depleted. The parent hydrocarbon was vaporized from a flask filled with pure substance by passing a constant flow of zero air regulated via a 0.1-10 $cm^3\ min^{-1}$ mass flow controller (Bronkhorst). HFA flow was regulated by another mass flow controller (Bronkhorst). Ozone was produced by passing zero air through an ozone generator using a low-pressure mercury ultraviolet lamp. Ozone concentration was measured using an ozone monitor (2B Technologies) (Table S2).

A proton-transfer-reaction mass spectrometer (PTR-8000, IONICON Analytik) was used to observe formed SCI·HFA adducts as well as parent hydrocarbons and their oxidation products. This instrument was operated using H_3O^+ reagent ions (H_3O^+ CIMS) and was directly calibrated to 10 VOCs with different functional groups (Isaacman-VanWertz et al., 2017; Isaacman-VanWertz et al., 2018).

2.2 Experiments with spin traps

2.2.1 Kinetics experiments with spin trap TEMPO

Highly reactive spin traps are needed for effective derivatization of radicals and reactive intermediates in the gas phase. A set of experiments, in which the reaction rate coefficient between the spin trap TEMPO ($C_9H_{18}NO$) and OH was measured, was conducted in a flow tube experimental setup at Forschungszentrum Jülich. TEMPO is commonly used to detect carbon-centered radicals in chemical and biological systems (Bagryanskaya and Marque, 2014) and is known to be highly reactive towards OH in the aqueous phase (Samuni et al., 2002). TEMPO was introduced in the flow tube setup using a liquid calibration unit (LCU, IONICON Analytik). The LCU quantitatively evaporates aqueous standards into the gas stream. TEMPO standard was prepared gravimetrically with aqueous volume mixing ratio of 485 parts per million (ppm). A known amount (up to 10 μL min^{-1}) of this solution was then evaporated into a humidified gas stream of synthetic air (31 SLPM), resulting in the gas-phase TEMPO concentration of up to 4.5×10^{11} molecule cm^{-3}. One part of the setup outflow was drawn to a laser photolysis – laser-induced fluorescence (LP-LIF) instrument (Lou et al., 2010), with which OH reactivity of TEMPO was measured. Laser flash photolysis of ozone was used to produce OH in the experimental setup, while LIF was applied to monitor the time dependent OH decay. Another part of the outflow was drawn to a CIMS instrument PTR3 (IONICON Analytik) to monitor concentrations of TEMPO and its oxidation products. This instrument was operated in two ionization modes: using $H_3O^+{\cdot}(H_2O)_n$, n = 0–1 (as H_3O^+ CIMS; Breitenlechner et al., 2017) and $NH_4^+{\cdot}(H_2O)_n$, n = 0–2 (as NH_4^+ CIMS; Zaytsev et al., 2019) reagent ions. The PTR3 is designed to minimize inlet losses of sampled compounds. It was directly calibrated to 10 VOCs with different functional groups using LCU. Collision-dissociation methods were used to constrain sensitivities of NH_4^+ CIMS to compounds that cannot be calibrated directly (Zaytsev et al., 2019). Sensitivities were calculated in normalized duty-cycle-corrected counts per second per part per billion by volume (ndcps ppb^{-1}; the duty-cycle correction was done to the reference *m/z* = 100; ion signals were normalized to the primary ion signal of 10^6 dcps).

2.2.2 Ozonolysis experiments with spin trap DMPO

An additional set of ozonolysis experiments of several hydrocarbons including TME and α-pinene were conducted in a double flow reactor setup (Fig. 2). The goal of these experiments was to examine how spin traps can be used for simultaneous detection of stabilized Criegee intermediates and peroxy radicals. Experimental setup consisted of two identical ~2.1L flow reactors. The parent hydrocarbon was mixed with ozone in the first flow tube reactor with a residence time of ~28s. Similar to the previous ozonolysis experiments described in Sect. 2.1, the parent hydrocarbon was vaporized from a flask filled with pure substance by passing zero air regulated by a mass flow controller, and ozone was generated using a low-pressure mercury ultraviolet lamp. ~~while the spin trap DMPO ($C_6H_{11}NO$) was introduced in the second flow tube using an LCU.~~ We used an LCU to introduce the spin trap DMPO ($C_6H_{11}NO$) in the second flow reactor with a residence time of ~23s. A known amount (up to 10 μL min^{-1}) of the DMPO solution was evaporated into a humidified gas stream of synthetic air (5.4-7 SLPM), resulting in the gas-phase DMPO concentration of up to 1.1×10^{13} molecule cm^{-3}. The second flow reactor served for derivatization of SCIs and RO_2 species by DMPO while the parent hydrocarbon was still reacting with ozone. Hence, we conducted integrated production measurements of SCIs and RO_2 species formed in both flow reactors. DMPO represents a class of non-radical spin traps and is widely used to detect oxygen-centered radicals, such as OH, HO_2 and RO_2, in chemical and biological systems (Roberts et al., 2016; Van Der Zee at al., 1996). Recently, DMPO was also employed to detect SCIs in the gas phase (Giorio et al., 2017). ~~Similar to the previous ozonolysis experiments described in Sect. 2.1, the parent hydrocarbon was vaporized from~~

~~a flask filled with pure substance by passing zero air regulated by a mass flow controller, and ozone was generated using a low-pressure mercury ultraviolet lamp.~~ The PTR3 was used ~~implemented~~ to detect SCI·DMPO and RO_2·DMPO adducts ~~spin trap adducts with SCIs and RO_2 species~~, while ozone levels were observed using an ozone monitor (2B Technologies) (Table S3).

2.3 Kinetic model and quantum-chemical calculations

The Framework for 0-D Atmospheric Modelling v3.1 (F0AM; Wolfe et al., 2016) containing reactions from the Master Chemical Mechanism (MCM v3.3.1) (Jenkin et al., 1997; Saunders et al., 2003) was used to simulate photooxidation of studied alkenes in the flow reactor system and to compare the modeled concentrations of the products with the measurements. Model calculations were constrained using physical parameters of the experimental setup (pressure and temperature) as well as to observed concentrations of the parent hydrocarbon, ozone and the chemical derivatization agent.

In order to estimate proton affinities of SCI·HFA adducts, we performed geometry optimization and proton affinity calculations with the Gaussian 09 package (Frisch et al., 2009) using the B3LYP functional (Stephens et al., 1994) and TZVP basis sets.

3 Results and discussion

3.1 Detection of speciated stabilized Criegee intermediates using chemical derivatization techniques

The primary goal of the first set of experiments was detection of speciated stabilized Criegee intermediates as adducts with the chemical derivatization agent HFA to prevent secondary reactions within the experimental setup. Starting with $(CH_3)_2COO$, an SCI produced via ozonolysis of TME, we tested the formation of SCI·HFA adducts under different experimental conditions (Fig. 3). $(CH_3)_2COO$·HFA ($C_6H_6O_3F_6 \cdot H^+$, *m/z* 241.03) can be easily identified in the mass-spectrum due to its unique mass defect associated with six F-atoms (Fig. S2). SCI·HFA adducts were observed when TME, ozone, and HFA were present in the experimental setup. Ozonolysis of TME also results in the formation of acetone ($C_3H_6O \cdot H^+$, *m/z* 59.05), which was detected in the presence of TME and ozone and was not affected by HFA addition (Fig. 3). ~~Since the reaction rate constant of SCI·HFA with H_3O^+ ions is unknown, we assumed that all SCI·HFA adducts were ionized via proton transfer from hydronium ions and therefore used the sensitivity we obtained from acetone calibration to quantify detected SCI·HFA species. In addition, we did not take into account possible fragmentation of SCI·HFA adducts which may impede their detection, although a first bond cleavage would likely only break the ozonide ring structure without loss of mass. These assumptions may lead to measurement uncertainties as discussed later in this section.~~

We measured the $(CH_3)_2COO$·HFA adduct signal as a function of different reactant conditions: initial TME concentration were in the range of $(1.48 - 1.85) \times 10^{11}$ molecule cm^{-3}, ozone, $(6.77 - 108.2) \times 10^{12}$ molecule cm^{-3}, HFA $(1.17 - 6.13) \times 10^{15}$ molecule cm^{-3}. The measurements are compared to the predictions of the kinetic model in Fig. 4. Concentrations of

$(CH_3)_2COO$ species were calculated using the MCM with updated kinetics data from the literature (Newland et al., 2015; Chhantyal-Pun et al., 2016; Long et al., 2018). For more details see the Supplement.

In the presence of HFA, SCI can react with HFA and form stable adducts:

$$(CH_3)_2COO + HFA \xrightarrow{k_1} (CH_3)_2COO{\cdot}HFA \qquad \text{(R1)}$$

The reaction rate coefficient k_1 was not measured experimentally, and we used the k-value for CH_2OO + HFA reaction: $k_1 = 3 \times 10^{-11}$ cm^3 molecule^{-1} s^{-1} (Taatjes et al., 2012). It has been suggested that the reaction between HFA and acetone oxide may be slower compared to the CH_2OO one (Murray et al., 1965; Taatjes et al., 2012) while $k_{(CH_3)_2COO+HFA} = 2 \times 10^{-13}$ molecule cm^{-3} s^{-1} was used in the previous studies (Drozd et al., 2011). However, the concentration of HFA was two orders of magnitude higher than concentrations of other chemical compounds, so even at lower k-values reaction with HFA remains the major chemical loss pathway for $(CH_3)_2COO$ (Fig. S3).

Observed concentrations of $(CH_3)_2COO{\cdot}HFA$ agree to within a factor of 3 with concentrations predicted by the kinetic model (Fig. 4). This discrepancy can be explained by a combination of the following factors. First, a fraction of $(CH_3)_2COO{\cdot}HFA$ adducts might be irreversibly deposited on the surfaces inside the experimental setup and the PTR 8000 instrument (Pagonis et al., 2017). ~~: (1) wall losses of $(CH_3)_2COO{\cdot}HFA$ in the experimental setup and the PTR 8000 instrument;~~ In addition, the sensitivity of observed SCI·HFA adducts depends on the reaction rate constant of the adduct with H_3O^+ ion and the degree of fragmentation of protonated product ions SCI·HFA·H^+ (Yuan et al., 2017). Since the reaction rate constant of SCI·HFA with H_3O^+ ions is unknown, we assumed that all SCI·HFA adducts were ionized via proton transfer from hydronium ions and therefore used the sensitivity we obtained from acetone calibration to quantify detected SCI·HFA species. In addition, we did not take into account possible fragmentation of SCI·HFA·H^+ ions which may impede their detection, although a first bond cleavage would likely only break the ozonide ring structure without loss of mass. ~~(2) uncertainty in the sensitivity at which the SCI·HFA adducts were detected; (3) potential ion fragmentation of protonated SCI·HFA adducts;~~ Finally, uncertainty of the kinetic model output is determined by the uncertainty in the SCI yield, and unimolecular and bimolecular reaction rate coefficients. ~~and (4) uncertainty in the SCI yield, and unimolecular and bimolecular reaction rate coefficients used in the kinetic model.~~ The detection limit for $(CH_3)_2COO{\cdot}HFA$ adducts was 1.4×10^7 molecule cm^{-3} and was calculated for 30 s integration time as 3 standard deviations of measured background divided by derived sensitivity.

Besides TME, we also observed formation of SCI·HFA for a series of precursors including isoprene, pentene, and hexene. (Figs. S4-S6). Proton affinities (PAs) of different CI·HFA adducts were calculated using DFT methods (Table 1). A variety of these adducts can be detected using H_3O^+ CIMS since their PAs are significantly higher than that of water which is in agreement with experimental data (Figs. S4-S6). $CH_2OO{\cdot}HFA$ cannot be detected because of its low PA (Table 1). We also did not observe SCI·HFA adducts for larger C_{10} SCIs produced via ozonolysis of α-pinene and limonene. This can be explained by the lower reactivity of larger SCIs with HFA, potential instability of these secondary ozonides in the gas phase, or their gas-wall partitioning in tubing and inside the PTR-8000 instrument.

3.2 Reactivity of spin traps with OH

Spin traps have been shown to be highly reactive towards free radicals and efficiently form adducts with them in the aqueous phase. However, their reactivity with atmospheric radicals and stability of formed adducts in the gas phase remain largely unknown. In order to address these questions, we conducted a set of experiments to estimate the reaction rate between the spin trap TEMPO and the hydroxyl radical by measuring its OH reactivity.

OH reactivity of a specific reactant can be calculated as a product of the reactant concentration and its reaction rate with OH (Fuchs et al., 2017):

$$k_{\mathrm{OH}} = k_{\mathrm{OH+TEMPO}} \cdot [\mathrm{TEMPO}] \quad (1)$$

k_{OH} was measured as a function of TEMPO concentration by varying the amount of TEMPO introduced in the experimental setup using the LCU (Fig. 5). The slope of the fitted line in Fig. 5 determines the reaction rate coefficient $k_{\mathrm{OH+TEMPO}} = (9.3 \pm 0.9) \times 10^{-11}$ cm^3 molecule^{-1} s^{-1}. This rate constant is close to the collisional limit of typical radical-molecule reactions in the atmosphere and is one order of magnitude greater than the rate constant for the same reaction in the aqueous phase ($k_{\mathrm{aqueous}} = 7.5 \times 10^{-12}$ cm^3 molecule^{-1} s^{-1}; Samuni et al., 2002). This demonstrates that TEMPO is highly reactive towards OH in the gas phase, emphasizing the applicability of spin trapping for atmospheric measurements. Furthermore, TEMPO + OH reaction leads to the formation of stable TEMPO·OH adducts that can be detected by H_3O^+ CIMS ($C_9H_{18}NO{\cdot}H^+$, *m/z* 174.149) and therefore could be used for quantification of hydroxyl radicals in the atmosphere (Fig. S7). Further tests are needed to compare the measurement capability of this method (e.g., sensitivity, wall losses, and potential interferences) with that of a well-established technique, such as LIF.

3.3 Simultaneous detection of SCIs and RO₂ species from ozonolysis of alkenes using spin trapping techniques

Next, we implemented spin trapping for detection of speciated SCIs and RO_2 species formed via ozonolysis of alkenes, starting with TME. Decomposition of the TME primary ozonide leads to formation of acetone oxide $(CH_3)_2COO$. This SCI can further undergo a unimolecular reaction followed by O_2 addition to form a peroxy radical $\mathrm{CH_3C(=O)CH_2OO^{\cdot}}$ and OH (Fig. 1). In order to detect SCIs and RO_2 species produced via ozonolysis of TME, we used a measurement method based on stabilization of these species using the spin trap DMPO followed by detection by NH_4^+ and H_3O^+ CIMS. DMPO was shown to form stable secondary ozonides with SCIs in the gas phase (Giorio et al., 2017):

$$\mathrm{(CH_3)_2COO + DMPO \rightarrow (CH_3)_2COO{\cdot}DMPO} \quad \mathrm{(R2)}$$

DMPO is shown to be highly reactive towards SCIs ($k_{\mathrm{CI+DMPO}} \geq 6 \times 10^{-11}$ cm^3 molecule^{-1} s^{-1}; see the Supplement for more details).

In addition, DMPO is known to be highly reactive towards oxygen-centered radicals, such as RO_2, and form stable radical adducts with them (Fig. 1):

$$\mathrm{CH_3C(=O)CH_2OO^{\cdot} + DMPO \rightarrow [CH_3C(=O)CH_2OO \cdot DMPO]^{\cdot}} \quad \mathrm{(R3)}$$

We observed the formation of SCI·DMPO and RO_2·DMPO adducts both in NH_4^+ CIMS (e.g., $C_9H_{17}NO_3 \cdot NH_4^+$, *m/z* 205.155 and $C_9H_{16}NO_4 \cdot NH_4^+$, *m/z* 220.142) and H_3O^+ CIMS (e.g., $C_9H_{17}NO_3 \cdot H^+$, *m/z* 188.128 and $C_9H_{16}NO_4 \cdot H^+$, *m/z* 203.116) under different experimental conditions (Figs. 6 and S8). SCI·DMPO and RO_2·DMPO were only detected when TME, ozone, and DMPO were present in the experimental setup. Acetone, also formed via ozonolysis of TME, was observed in the presence of TME and ozone and was not affected by addition of DMPO (Figs. 6 and S8). OH radicals, formed via decomposition of SCI, can in turn react with TME and lead to formation of another RO_2 species OH-$C_6H_{12}OO\cdot$. This radical was detected as the $C_6H_{13}O_3$·DMPO adduct ($C_{12}H_{24}NO_4$, m/z 264.205; Fig. 6). One of the benefits of NH_4^+ CIMS is the possibility of quantifying compounds for which authentic standards are not available, using a voltage scanning procedure based on collision-induced dissociation (Zaytsev et al., 2019). Based on this method, DMPO adducts with SCIs and RO_2 were detected at high sensitivities: 2,400 ndcps $ppbv^{-1}$ for SCI·DMPO and 2,000 ndcps $ppbv^{-1}$ for RO_2·DMPO (Table S1). Sensitivities were experimentally determined in each ozonolysis experiment and depend on the operational conditions of the PTR3 instrument. Detection limits for SCI·DMPO and RO_2·DMPO adducts were 3.4×10^7 and 1.6×10^8 molecule cm^{-3}, respectively. These limits of detection are calculated for 30 s integration time as 3 standard deviations of measured background divided by derived sensitivity.

In addition, we compare measured concentrations of RO_2·DMPO adducts with the concentrations predicted by the kinetic model (Fig. 7). The observed values are an order of magnitude lower than the modeled ones. Similar to experiments described in Sect. 3.1, several factors can contribute to this discrepancy: (1) gas-wall partitioning of RO_2 species and RO_2·DMPO adducts in the experimental setup ~~flow tube setup~~ and inside the PTR3 instrument; (2) uncertainty in sensitivity at which RO_2·DMPO adducts were detected; (3) potential fragmentation of $RO_2 \cdot DMPO \cdot NH_4^+$ product ions; and (4) uncertainties in the reaction rate coefficient $k_{\mathrm{RO_2+DMPO}}$. In our model we assumed that the major fraction of RO_2 species was scavenged by DMPO. This assumption is valid if $k_{\mathrm{RO_2+DMPO}}$ is larger than 1×10^{-12} cm^3 $molecule^{-1}$ s^{-1}. Otherwise, other loss channels for peroxy radicals, especially the RO_2+RO_2 reaction, become more important (Fig. S9). Additional experiments under different conditions and intercomparison with established methods (i.e., LIF) are needed to further estimate the measurement capability of the proposed analytical method.

Finally, we employed spin trapping for detection of SCIs and organic peroxy radicals formed via ozonolysis of larger cyclic alkenes, such as α-pinene. Decomposition of the α-pinene primary ozonide yields four different C_{10}-SCIs, all of which have the same molecular formula $C_{10}H_{16}O_3$ (Newland et al., 2018). These SCIs can further isomerize to form primary peroxy radicals $C_{10}H_{15}O_4$ and OH. Autoxidation of $C_{10}H_{15}O_4$-RO_2 species can in turn result in formation of several more oxygenated peroxy radicals $C_{10}H_{15}O_x$, x = 5-9 (Zhao et al., 2018). Signals of SCI·DMPO ($C_{10}H_{16}O_3$·DMPO) and RO_2·DMPO ($C_{10}H_{15}O_x$·DMPO, x = 4-9) adducts were observed both in NH_4^+ and H_3O^+ CIMS (Figs. 8, S10, S11). OH radicals, formed via decomposition of SCI, can in turn react with α-pinene and lead to formation of OH-derived RO_2 species $C_{10}H_{17}O_3$ and subsequent autoxidation RO_2 species $C_{10}H_{17}O_5$ (Berndt et al., 2016). These radicals were detected as the RO_2·DMPO adducts (Figs. S10 and S11). This demonstrates that this analytical method allows for simultaneous detection of a wide range of atmospheric radicals, including the ones with high oxygen content (an O:C ration of up to 0.9) that are formed via autoxidation pathway, and can be used to study kinetics of these species in the laboratory.

4 Conclusions

In summary, we experimentally demonstrated the measurement of speciated, short-lived highly reactive atmospheric compounds, such as Criegee intermediates, organic peroxy radicals and hydroxyl radicals, formed via ozonolysis of alkenes. The analysis was carried out using chemical derivatization techniques, including spin trapping, while the detection of formed radical adducts and closed-shell secondary ozonides was performed by the means of H_3O^+ and NH_4^+ CIMS. Detected adducts and secondary ozonides have unique mass defects and can therefore be clearly separated from other observed compounds in the mass spectrum. Implementation of chemical derivatization agents with lower proton affinity allows for the full scavenging and quantification of stabilized Criegee intermediates without depleting CIMS reagent ions. We show that spin traps can be used to effectively scavenge atmospheric radicals and reactive intermediates by demonstrating their high reactivity with radicals in the gas phase using the TEMPO+OH reaction as an example. Using the spin trap DMPO, SCIs and RO_2 species can be simultaneously detected while quantification of observed adducts can be done without their direct calibration. The detection limits of spin trap and chemical derivatization agent adducts of 1.4×10^7 molecule cm^{-3} for SCIs and 1.6×10^8 molecule cm^{-3} for RO_2 for 30 s integration time were estimated for the instrumentation used here and show promise that these techniques would also work when sampling ambient air. In particular, this method fundamentally enables any CIMS instrument to detect radicals and SCIs. Since spin traps, such as DMPO and TEMPO, are reactive towards a plethora of atmospheric radicals and reactive intermediates, including RO_2, SCIs, and OH, implementation of such spin traps results in the effective suppression of the radical secondary chemistry and, thus, elimination of potential chemical interferences. The direct method for speciated SCIs and RO_2 measurements provides a means to study the atmospheric chemistry of these compounds. We stress that the quantification of RO_2 species was done under well-defined laboratory conditions using the CID technique such that the estimated sensitivities are likely unique to the electric fields, pressures and flows of the NH_4^+ CIMS instrument. Further validation of the proposed analytical methods in more complex environments closer to the ambient conditions and intercomparison with established methods (i.e., LIF) are needed.

For the future application of the method in field and laboratory experiments, various modifications of the experimental setup can be implemented to improve its measurement capability. We plan to synthesize and test new chemical derivatization agents optimized for the gas-phase measurements with respect to their vapor pressure, selective reactivity and by labelling with atomic isotopes to simplify mass spectrometric detection and improve detection limits. With labeled spin traps, the identification of reactive intermediates may be greatly simplified and detection limits may be further improved, as the spin trap can provide a unique signature in the complex mass-spectrum and move the observed *m/z* to a region with very low background.

Acknowledgements. This work has received funding from the Harvard Global Institute. Martin Breitenlechner acknowledges support from the Austrian science fund (FWF; grant J-3900). Hendrik Fuchs and Anna Novelli acknowledge support from the European Research Council (ERC) under the European Union's Horizon 2020 research and innovation programme (SARLEP grant agreement No. 681529). Daniel Knopf acknowledges support from the U.S. National Science Foundation (grant no. AGS-1446286). Jesse Kroll acknowledges support from the U.S. National Science Foundation (grant no. AGS-1638672).

References

Bagryanskaya, E.G. and Marque, S.R.: Scavenging of organic C-centered radicals by nitroxides. Chem. Rev., 114(9), 5011-5056, DOI: 10.1021/cr4000946, 2014.

Berndt, T., Jokinen, T., Sipilä, M., Mauldin III, R.L., Herrmann, H., Stratmann, F., Junninen, H. and Kulmala, M.: H_2SO_4 formation from the gas-phase reaction of stabilized Criegee Intermediates with SO_2: Influence of water vapour content and temperature. Atmospheric Environment, 89, 603-612, DOI: 10.1016/j.atmosenv.2014.02.062, 2014.

Berndt, T., Richters, S., Jokinen, T., Hyttinen, N., Kurtén, T., Otkjær, R.V., Kjaergaard, H.G., Stratmann, F., Herrmann, H., Sipilä, M., Kulmala, M., and Ehn, M.: Hydroxyl radical-induced formation of highly oxidized organic compounds, Nature Communications, 7, 13677, DOI: 10.1038/ncomms13677, 2016.

Berndt, T., Herrmann, H., and Kurten, T.: Direct Probing of Criegee Intermediates from Gas-Phase Ozonolysis Using Chemical ionization Mass Spectrometry, J. Am. Chem. Soc., 139, 13387-13392, DOI: 10.1021/jacs.7b05849, 2017.

Berndt, T., Mentler, B., Scholz, W., Fischer, L., Herrmann, H., Kulmala, M. and Hansel, A.: Accretion product formation from ozonolysis and OH radical reaction of α-pinene: mechanistic insight and the influence of isoprene and ethylene. Environmental science & technology, 52(19), 11069-11077, DOI: 10.1021/acs.est.8b02210, 2018.

Berndt, T., Hyttinen, N., Herrmann, H., and Hansel, A.: First oxidation products from the reaction of hydroxyl radicals with isoprene for pristine environmental conditions. Communications Chemistry, 2(1), 1-10, DOI: 10.1038/s42004-019-0120-9, 2019.

Breitenlechner, M., Fischer, M., Hainer, M., Heinritzi, M., Curtius, M., and Hansel, A.: PTR3: An instrument for Studying the Lifecycle of Reactive Organic Carbon in the Atmosphere, Anal. Chem., 89, 5824–5831, DOI: 10.1021/acs.analchem.6b05110, 2017.

Cantrell, C.A., Stedman, D.H., and Wendel, G.J.: Measurement of atmospheric peroxy radicals by chemical amplification, Anal. Chem., 56, 1496–1502. DOI: 10.1021/ac00272a065, 1984.

Chhantyal-Pun, R., Welz, O., Savee, J.D., Eskola, A.J., Lee, E.P.F., Blacker, L., Hill, H.R., Ashcroft, M., Khan, M.A.H., Lloyd-Jones, G.C., Evans, L., Rotavera, B., Huang, H., Osborn, D.L., Mok, D.K.W., Dyke, J.M., Shallcross, D.E., Percival. C.J., Orr-Ewing, A.J., and Taatjes, C.A.: Direct Measurements of Unimolecular and Bimolecular Reaction Kinetics of the Criegee Intermediate $(CH_3)_2COO$, J. Phys. Chem. A, 121, 4−15, DOI: 10.1021/acs.jpca.6b07810, 2016.

Drozd, G.T., Kroll, J.H., and Donahue, N.M.: 2,3-Dimethyl-2-butene (TME) Ozonolysis: Pressure Dependence of Stabilized Criegee Intermediates and Evidence of Stabilized Vinyl Hydroperoxides, J. Phys. Chem. A, DOI: 10.1021/jp108773d, 2011.

Drozd, G.T. and Donahue, N.M.: Pressure Dependence of Stabilized Criegee Intermediate Formation from a Sequence of Alkenes, J. Phys. Chem. A, DOI: 10.1021/jp2001089, 2011.

Edwards, G.D., Cantrell, C.A., Stephens, S., Hill, B., Goyea, O., Shetter, R.E., Mauldin III, R.L., Kosciuch, E., Tanner, D.J., and Eisele, F.L.: Chemical Ionization Mass Spectrometer Instrument for the Measurement of Tropospheric HO_2 and RO_2, Anal. Chem., 75, 5317-5327, DOI: 10.1021/ac034402b, 2003.

Frisch, M. J., Trucks, G. W., Schlegel, H. B., Scuseria, G. E., Robb, M. A., Cheeseman, J. R., Scalmani, G., Barone, V., Mennucci, B., Petersson, G. A., Nakatsuji, H., Caricato, M., Li, X., Hratchian, H. P., Izmaylov, A. F., Bloino, J., Zheng, G., Sonnenberg, J. L., Hada, M., Ehara, M., Toyota, K., Fukuda, R., Hasegawa, J., Ishida, M., Nakajima, T., Honda, Y., Kitao, O., Nakai, H., Vreven, T., Montgomery, J. A., Jr., Peralta, J. E., Ogliaro, F., Bearpark, M., Heyd, J. J., Brothers, E., Kudin, K. N., Staroverov, V. N., Kobayashi, R., Normand, J., Raghavachari, K., Rendell, A., Burant, J. C., Iyengar, S. S., Tomasi, J., Cossi, M., Rega, N., Millam, J. M., Klene, M., Knox, J. E., Cross, J. B., Bakken, V., Adamo, C., Jaramillo, J., Gomperts, R., Stratmann, R. E., Yazyev, O., Austin, A. J., Cammi, R., Pomelli, C., Ochterski, J. W., Martin, R. L., Morokuma, K., Zakrzewski, V. G., Voth, G. A., Salvador, P., Dannenberg, J. J., Dapprich, S., Daniels, A. D., Farkas, Ö., Foresman, J. B., Ortiz, J. V., Cioslowski, J., and Fox, D. J.: Gaussian 09, Revision D.01, Gaussian, Inc.: Wallingford, CT, 2009.

Fuchs, H., Holland, F., and Hofzumahaus, A.: Measurement of tropospheric RO_2 and HO_2 radicals by a laser-induced fluorescence instrument, Rev. Sci. Instrum., 79, 084104, DOI: 10.1063/1.2968712, 2008.

Fuchs, H., Novelli, A., Rolletter, M., Hofzumahaus, A., Pfannerstill, E. Y., Kessel, S., Edtbauer, A., Williams, J., Michoud, V., Dusanter, S., Locoge, N., Zannoni, N., Gros, V., Truong, F., Sarda-Esteve, R., Cryer, D. R., Brumby, C. A., Whalley, L. K., Stone, D., Seakins, P. W., Heard, D. E., Schoemaecker, C., Blocquet, M., Coudert, S., Batut, S., Fittschen, C., Thames, A. B., Brune, W. H., Ernest, C., Harder, H., Muller, J. B. A., Elste, T., Kubistin, D., Andres, S., Bohn, B., Hohaus, T., Holland, F., Li, X., Rohrer, F., Kiendler-Scharr, A., Tillmann, R., Wegener, R., Yu, Z., Zou, Q., and Wahner, A.: Comparison of OH reactivity measurements in the atmospheric simulation chamber SAPHIR, Atmos. Meas. Tech., 10, 4023–4053, DOI: 10.5194/amt-10-4023-2017, 2017.

Giorio, C., Campbell, S.J., Bruschi, M., Tampieri, F., Barbon, A., Toffoletti, A., Tapparo, A., Paijens, C., Wedlake, A.J., Grice, P., Howe, D.J., and Kalberer, M.: Online Quantification of Criegee Intermediates of α-Pinene Ozonolysis by Stabilization with Spin Traps and Proton-Transfer Reaction Mass Spectrometry Detection, J. Am. Chem. Soc., 139, 3999−4008, DOI: 10.1021/jacs.6b10981, 2017.

Hansel, A., Scholz, W., Mentler, B., Fischer, L. and Berndt, T.: Detection of RO_2 radicals and other products from cyclohexene ozonolysis with NH_4^+ and acetate chemical ionization mass spectrometry. Atmospheric Environment, 186, 248-255, DOI: 10.1016/j.atmosenv.2018.04.023, 2018.

Hawkins, C.L. and Davies, M.J.: Detection and characterisation of radicals in biological materials using EPR methodology, Biochimica et Biophysica Acta (BBA)-General Subjects, 1840(2), 708-721, DOI: 10.1016/j.bbagen.2013.03.034, 2014.

Horie, O., Schäfer, C. and Moortgat, G.K.: High reactivity of hexafluoro acetone toward criegee intermediates in the gas-phase ozonolysis of simple alkenes. International journal of chemical kinetics, 31(4), 261-269, DOI: 10.1002/(SICI)1097-4601(1999)31:4<261::AID-KIN3>3.0.CO;2-Z, 1999.

Hornbrook, R.S., Crawford, J.H., Edwards, G.D., Goyea, O., Mauldin Iii, R.L., Olson, J.S., Cantrell, C.A: Measurements of tropospheric HO_2 and RO_2 by oxygen dilution modulation and chemical ionization mass spectrometry. Atmos Meas Tech 4, 735–756. DOI: 10.5194/amt-4-735-2011, 2011.

Hunter, E.P. and Lias, S.G.: Evaluated Gas Phase Basicities and Proton Affinities of Molecules: An Update, J. Phys. Chem. Ref. Data, 27, 3, 413-656, DOI: 10.1063/1.556018, 1998.

Isaacman-VanWertz, G., Massoli, P., O'Brien, R.E., Nowak, J.B., Canagaratna, M.R., Jayne, J.T., Worsnop, D.R., Su, L., Knopf, D.A., Misztal, P.K., Arata, C., Goldstein, A.H. and Kroll, J.H.: Using advanced mass spectrometry techniques to fully characterize atmospheric organic carbon: current capabilities and remaining gaps. Faraday Discussions, 200, 579-598, DOI: 10.1039/c7fd00021a, 2017.

Isaacman-VanWertz, G., Massoli, P., O'Brien, R., Lim, C., Franklin, J.P., Moss, J.A., Hunter, J.F., Nowak, J.B., Canagaratna, M.R., Misztal, P.K., Arata, C., Roscioli, J.R., Herndon, S.T., Onasch, T.B., Lambe, A.T., Jayne, J.T., Su, L., Knopf, D.A., Goldstein, A.H., Worsnop, D.R. and Kroll, J.H.: Chemical evolution of atmospheric organic carbon over multiple generations of oxidation. Nature Chem., 10, 462-468, DOI: 10.1038/s41557-018-0002-2, 2018.

Jenkin, M.E., Saunders, S.M., Pilling, M.J.: The tropospheric degradation of volatile organic compounds: a protocol for mechanism development, Atmos. Environ., 31, 81-104, DOI: 10.1016/S1352-2310(96)00105-7, 1997.

Johnson, D. and Marston, G.: The gas-phase ozonolysis of unsaturated volatile organic compounds in the troposphere. Chemical Society Reviews, 37(4), 699-716, DOI: 10.1039/b704260b, 2008.

Khan, M.A.H., Percival, C.J., Caravan, R.L., Taatjes, C.A. and Shallcross, D.E.: Criegee intermediates and their impacts on the troposphere, Environ. Sci.: Processes Impacts, 20, 437, DOI: 10.1039/C7EM00585G, 2018.

Lewis, T.R., Blitz, M.A., Heard, D.E. and Seakins, P.W.: Direct evidence for a substantive reaction between the Criegee intermediate, CH_2OO, and the water vapour dimer. Physical Chemistry Chemical Physics, 17(7), 4859-4863, DOI: 10.1039/C4CP04750H, 2015.

Long, B., Bao, J.L., and Truhlar, D.G. Unimolecular reaction of acetone oxide and its reaction with water in the atmosphere, PNAS, 115, 6135-6140, DOI: 10.1073/pnas.1804453115, 2018.

Lou, S., Holland, F., Rohrer, F., Lu, K., Bohn, B., Brauers, T., Chang, C. C., Fuchs, H., Häseler, R., Kita, K., Kondo, Y., Li, X., Shao, M., Zeng, L., Wahner, A., Zhang, Y., Wang, W., and Hofzumahaus, A.: Atmospheric OH reactivities in the Pearl River Delta – China in summer 2006: measurement and model results, Atmos. Chem. Phys., 10, 11243–11260, https://doi.org/10.5194/acp-10-11243-2010, 2010.

Mihelcic, D., Müsgen, P., and Ehhalt, D.H.: An improved method of measuring tropospheric NO_2 and RO_2 by matrix isolation and electron spin resonance, J. Atmos. Chem., 3, 341-361, DOI: 10.1007/BF00122523, 1985.

Murray, R.W., Story, P.R., and Loan, L.D.: Ozonides from Aldehydic Zwitterions and Acetone, J. Am. Chem. Soc. 87, 13, 3025-3026, DOI: 10.1021/ja01091a054, 1965.

Neeb, P., Sauer, F., Horie, O., and Moortgat, G. K.: Formation of hydroxymethyl hydroperoxide and formic acid in alkene ozonolysis in the presence of water vapour, Atmos. Environ., 31, 1417– 1423, DOI: 10.1016/S1352-2310(96)00322-6, 1997.

Newland, M.J., Rickard, A.R., Alam, M.S., Vereecken, L., Munoz, A., Rodenasd, M. and Bloss, W.J.: Kinetics of stabilised Criegee intermediates derived from alkene ozonolysis: reactions with SO_2, H_2O and decomposition under boundary layer conditions. Phys. Chem. Chem. Phys., 17, 4076-4088, DOI: 10.1039/C4CP04186K, 2015.

Newland, M. J., Rickard, A. R., Sherwen, T., Evans, M. J., Vereecken, L., Muñoz, A., Ródenas, M., and Bloss, W. J.: The atmospheric impacts of monoterpene ozonolysis on global stabilised Criegee intermediate budgets and SO_2 oxidation: experiment, theory and modelling, Atmos. Chem. Phys., 18, 6095–6120, DOI: 10.5194/acp-18-6095-2018, 2018.

Nosaka, Y. and Nosaka, A.Y.: Generation and detection of reactive oxygen species in photocatalysis, Chem. Rev., 117(17), 11302-11336, DOI: 10.1021/acs.chemrev.7b00161, 2017.

Novelli, A., Hens, K., Tatum Ernest, C., Martinez, M., Nölscher, A. C., Sinha, V., Paasonen, P., Petäjä, T., Sipilä, M., Elste, T., Plass-Dülmer, C., Phillips, G. J., Kubistin, D., Williams, J., Vereecken, L., Lelieveld, J., and Harder, H.: Estimating the atmospheric concentration of Criegee intermediates and their possible interference in a FAGE-LIF instrument, Atmos. Chem. Phys., 17, 7807–7826, DOI: 10.5194/acp-17-7807-2017, 2017.

Nozière, B. and Vereecken, L.: Direct Observation of Aliphatic Peroxy Radical Autoxidation and Water Effects: An Experimental and Theoretical Study. Angew. Chem., 58(39), 13976-13982, DOI: 10.1002/anie.201907981, 2019.

Orlando, J.J., and Tyndall, G.S.: Laboratory studies of organic peroxy radical chemistry: an overview with emphasis on recent issues of atmospheric significance, Chem. Soc. Rev., 41, 6294–6317, DOI: 10.1039/c2cs35166h, 2012.

Pattison, D.I., Lam, M., Shinde, S.S., Anderson, R.F. and Davies, M.J.: The nitroxide TEMPO is an efficient scavenger of protein radicals: Cellular and kinetic studies. Free Radical Biology and Medicine, 53, 1664–1674, DOI: 10.1016/j.freeradbiomed.2012.08.578, 2012.

Pagonis, D., Krechmer, J. E., de Gouw, J., Jimenez, J. L., and Ziemann, P. J.: Effects of gas–wall partitioning in Teflon tubing and instrumentation on time-resolved measurements of gas-phase organic compounds, Atmos. Meas. Tech., 10, 4687–4696, DOI: 10.5194/amt-10-4687-2017, 2017.

Reiner, T., Hanke, M. and Arnold, F.: Atmospheric peroxy radical measurements by ion molecule reaction-mass spectrometry: A novel analytical method using amplifying chemical conversion to sulfuric acid. Journal of Geophysical Research: Atmospheres, 102(D1), 1311-1326, DOI: 10.1029/96JD02963, 1997.

Roberts, J.G., Voinov, M.A., Schmidt, A.C., Smirnova, T.I. and Sombers, L.A.: The hydroxyl radical is a critical intermediate in the voltammetric detection of hydrogen peroxide. J. Am. Chem. Soc., 138(8), 2516-2519, DOI: 10.1021/jacs.5b13376, 2016.

Samuni, A., Goldstein, S., Russo, A., Mitchell, J.B., Krishna, M.C. and Neta, P.: Kinetics and mechanism of hydroxyl radical and OH-adduct radical reactions with nitroxides and with their hydroxylamines. J. Am. Chem. Soc., 124(29), 8719-8724, DOI: 10.1021/ja017587h, 2002.

Saunders, S. M., Jenkin, M. E., Derwent, R. G., and Pilling, M. J.: Protocol for the development of the Master Chemical Mechanism, MCM v3 (Part A): tropospheric degradation of non-aromatic volatile organic compounds, Atmos. Chem. Phys., 3, 161–180, DOI: 10.5194/acp-3-161-2003, 2003.

Sipilä, M., Jokinen, T., Berndt, T., Richters, S., Makkonen, R., Donahue, N. M., Mauldin III, R. L., Kurtén, T., Paasonen, P., Sarnela, N., Ehn, M., Junninen, H., Rissanen, M. P., Thornton, J., Stratmann, F., Herrmann, H., Worsnop, D. R., Kulmala, M., Kerminen, V.-M., and Petäjä, T.: Reactivity of stabilized Criegee intermediates (sCIs) from isoprene and monoterpene ozonolysis toward SO_2 and organic acids, Atmos. Chem. Phys., 14, 12143–12153, DOI: 10.5194/acp-14-12143-2014, 2014.

Stephens, P. J., Devlin, F. J., Chabalowski, C. F. N., and Frisch, M. J.: Ab initio calculation of vibrational absorption and circular dichroism spectra using density functional force fields. The Journal of physical chemistry, 98, 11623-11627, DOI: 10.1021/j100096a001, 1994.

Taatjes, C.A., Meloni, G., Selby, T.M., Trevitt, A.J., Osborn, D.L., Percival, C.J. and Shallcross, D.E.: Direct observation of the gas-phase Criegee intermediate (CH_2OO). J. Am. Chem. Soc., 130(36), 11883-11885, DOI: 10.1021/ja804165q, 2008.

Taatjes, C.A., Welz, O., Eskola, A.J., Savee, J.D., Osborn, D.L., Lee, E.P.F., Dyke, J.M., Mok, D.W.K., Shallcross D.E., and Percival, C.J.: Direct measurement of Criegee intermediate (CH_2OO) reactions with acetone, acetaldehyde, and hexafluoroacetone, Phys. Chem. Chem. Phys., 14, 10391–10400, DOI: 10.1039/C2CP40294G, 2012.

Van Der Zee, J., Barr, D.P. and Mason, R.P.: ESR spin trapping investigation of radical formation from the reaction between hematin and tert-butyl hydroperoxide. Free Radical Biology and Medicine, 20(2), 199-206, DOI: 10.1016/0891-5849(95)02031-4, 1996.

Vereecken, L., Novelli, A. and Taraborrelli, D.: Unimolecular decay strongly limits the atmospheric impact of Criegee intermediates. Phys. Chem. Chem. Phys., 19(47), 31599-31612, DOI: 10.1039/C7CP05541B, 2017.

Watanabe, T., Yoshida, M., Fujiwara, S., Abe, K., Onoe, A., Hirota, M. and Igarashi, S.: Spin trapping of hydroxyl radical in the troposphere for determination by electron spin resonance and gas chromatography/mass spectrometry. Anal. Chem., 54(14), 2470-2474, DOI: 10.1021/ac00251a015, 1982.

Welz, O., Savee, J.D., Osborn, D.L., Vasu, S.S., Percival, C.J., Shallcross, D.E., and Taatjes, C.A.: Direct kinetic measurements of Criegee intermediate (CH_2OO) formed by reaction of CH_2I with O_2, Science, 335, 204-207, DOI: 10.1126/science.1213229, 2012.

Wolfe, G. M., Marvin, M. R., Roberts, S. J., Travis, K. R., and Liao, J.: The Framework for 0-D Atmospheric Modeling (F0AM) v3.1, Geosci. Model Dev., 9, 3309–3319, DOI: 10.5194/gmd-9-3309-2016, 2016.

Womack, C.C., Martin-Drumel, M.A., Brown, G.G., Field, R.W. and McCarthy, M.C.: Observation of the simplest Criegee intermediate CH_2OO in the gas-phase ozonolysis of ethylene. Sci. Adv., 1(2), DOI: 10.1126/sciadv.1400105, 2015.

Wood, E.C. and Charest, J.R.: Chemical amplification - cavity attenuated phase shift spectroscopy measurements of atmospheric peroxy radicals. Anal. Chem. 86, 10266–10273. DOI: 10.1021/ac502451m, 2014.

Wright, P.J. and English, A.M.: Scavenging with TEMPO• to identify peptide-and protein-based radicals by mass spectrometry: Advantages of spin scavenging over spin trapping. Journal of the American Chemical Society, 125(28), 8655-8665, DOI: 10.1021/ja0291888, 2003.

Yuan, B., Koss, A.R., Warneke, C., Coggon, M., Sekimoto, K., and de Gouw, J.A.: Proton-Transfer-Reaction Mass Spectrometry: Applications in Atmospheric Sciences, Chem. Rev., 117, 13187–13229, DOI: 10.1021/acs.chemrev.7b00325, 2017.

Zaytsev, A., Breitenlechner, M., Koss, A. R., Lim, C. Y., Rowe, J. C., Kroll, J. H., and Keutsch, F. N.: Using collision-induced dissociation to constrain sensitivity of ammonia chemical ionization mass spectrometry (NH_4^+ CIMS) to oxygenated volatile organic compounds, Atmos. Meas. Tech., 12, 1861–1870, DOI: 10.5194/amt-12-1861-2019, 2019.

Zhao, Y., Thornton, J.A., and Pye, H.O.: Quantitative constraints on autoxidation and dimer formation from direct probing of monoterpene-derived peroxy radical chemistry. Proceedings of the National Academy of Sciences, 115, 12142-12147, DOI: 10.1073/pnas.1812147115, 2018.

Table 1: Proton affinities (PAs) of HFA, water and secondary ozonides produced in reactions of SCIs with HFA. Species with PAs higher than that of water can be detected in H_3O^+ CIMS.

Species	PA, kcal/mol	Reference
$CH_2OO{\cdot}HFA$	662.9	This work
HFA	670.4	Hunter and Lias (1998)
H_2O	691	Hunter and Lias (1998)
$CH_3CH_2CHOO{\cdot}HFA$	720.7	This work
$CH_3CH_2CH_2CHOO{\cdot}HFA$	730.8	This work
$(CH_3)_2COO{\cdot}HFA$	747.2	This work
$(CH_2{=}C(CH_3))CHOO{\cdot}HFA$	779.6	This work

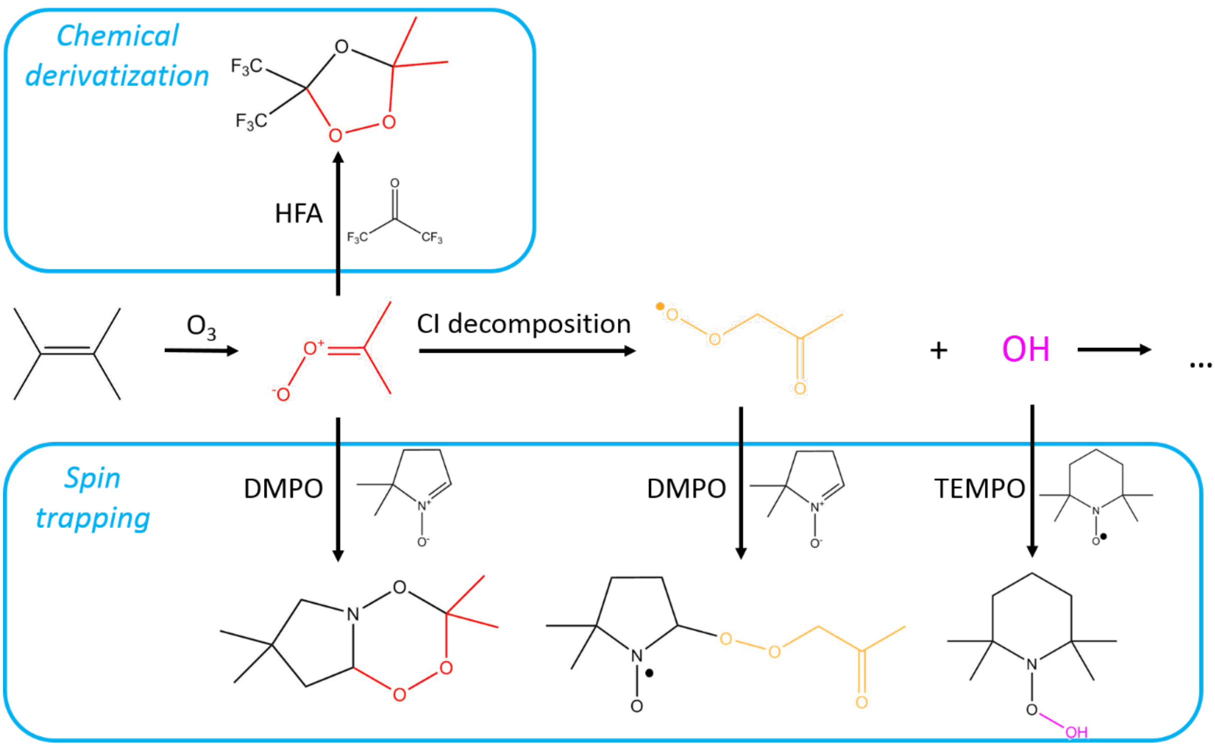

Figure 1: Mechanism of tetramethylethylene (TME) ozonolysis. Stabilized Crigee intermediate (shown in red) can be scavenged by the chemical derivatization agent HFA or the spin trap DMPO, or decompose to peroxy radical (shown in yellow) and OH. RO_2 and OH species can in turn react with spin traps. Reactions involving SCI are from MCM v3.3.1 (Jenkin et al., 1997) and Giorio et al. (2017).

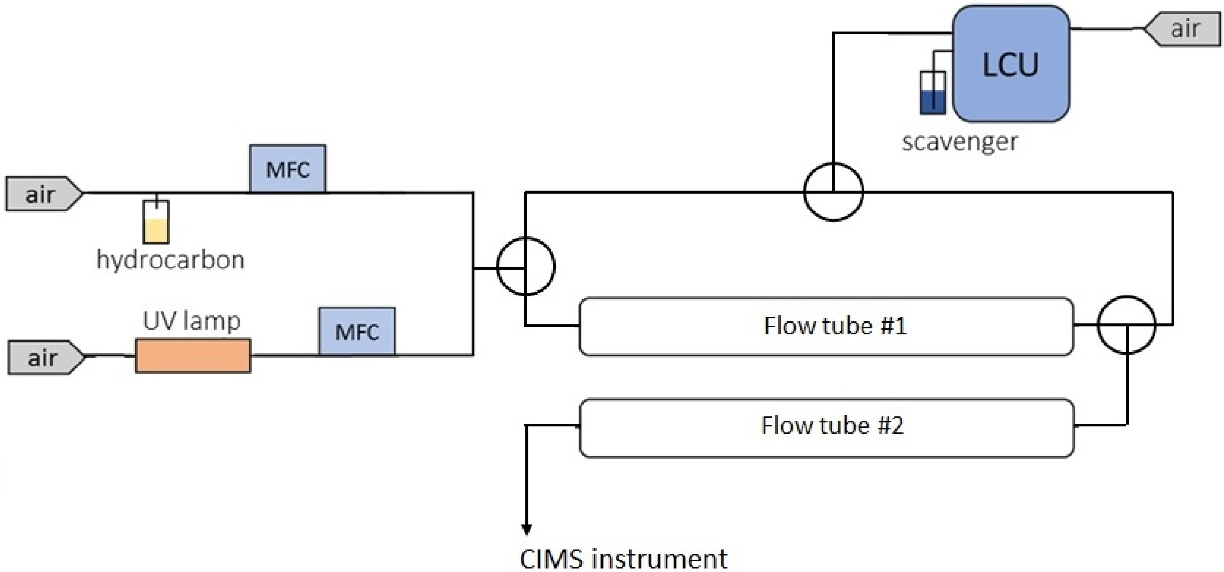

Figure 2: Schematic of experimental setup used to detect SCIs and RO_2 with the spin trap DMPO. DMPO was introduced in the experimental setup using a liquid calibration unit (LCU, IONICON Analytik).

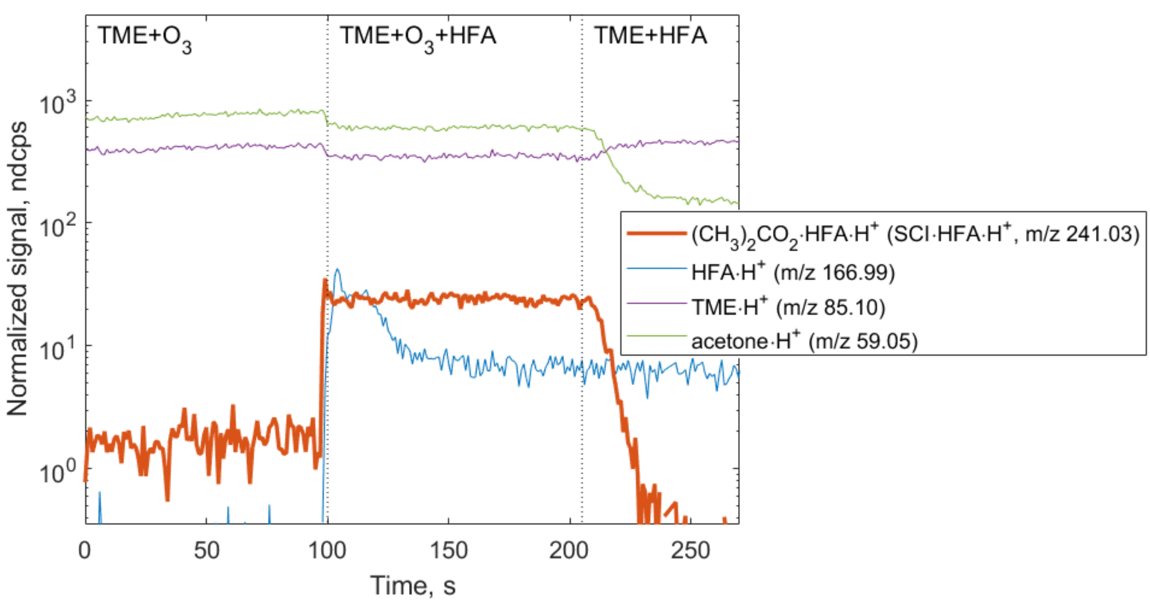

Figure 3: Ion tracers observed in a TME ozonolysis experiment as a function of different reactant conditions. Reactant concentrations are [TME] = 1.85×10^{12}; [O_3] = 1.67×10^{13}; [HFA] = 6.09×10^{15} molecule cm^{-3}. $(CH_3)_2COO \cdot HFA \cdot H^+$ ion (red tracer, *m/z* 241.03) is observed when TME, HFA, and O_3 are present in the system.

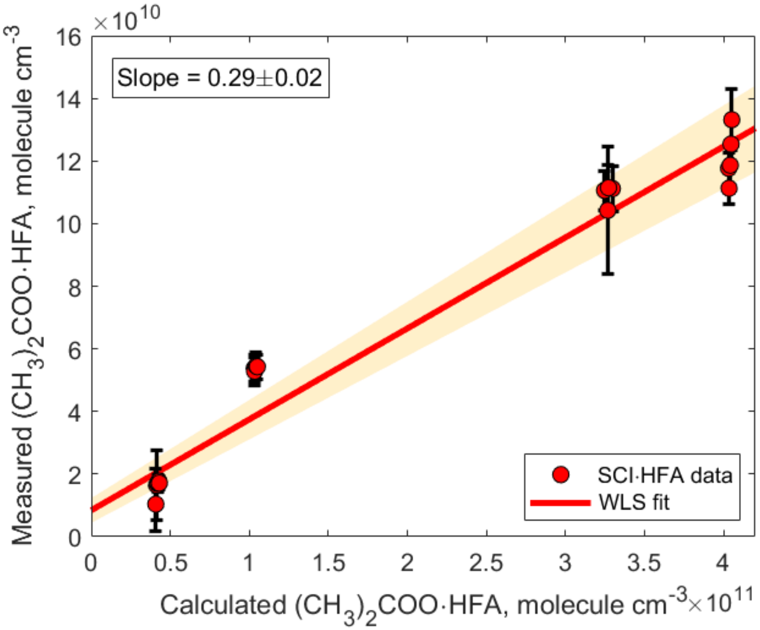

Figure 4: Correlation plot comparing measured and calculated concentrations of $(CH_3)_2COO{\cdot}HFA$. The adducts were detected using H_3O^+ CIMS as $(CH_3)_2COO{\cdot}HFA{\cdot}H^+$ (*m/z* 241.03). The slope is calculated using weighted least squares (WLS). A 95% confidence interval is estimated via a Monte Carlo simulation (N=5000) and shown using red shading.

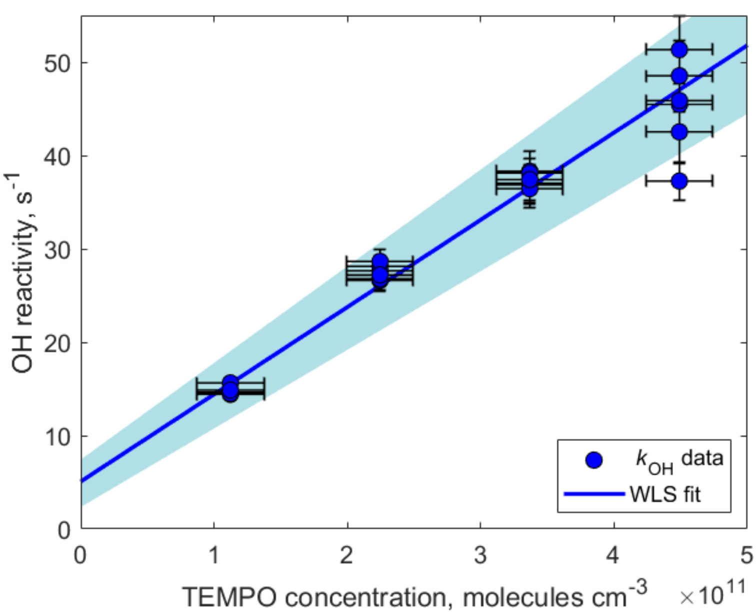

Figure 5: OH reactivity measured as a function of TEMPO concentration. The slope determining the reaction rate coefficient $k_{\mathrm{TEMPO+OH}} = (9.3 \pm 0.9) \times 10^{-11}$ cm^3 molecule^{-1} s^{-1} is calculated using weighted least squares (WLS). A 95% confidence interval is estimated via a Monte Carlo simulation (N=5000) and shown using blue shading. The intercept (5.1±2.4) s^{-1} can be explained by other OH reactants such as O_3, NO, NO_2, and CO.

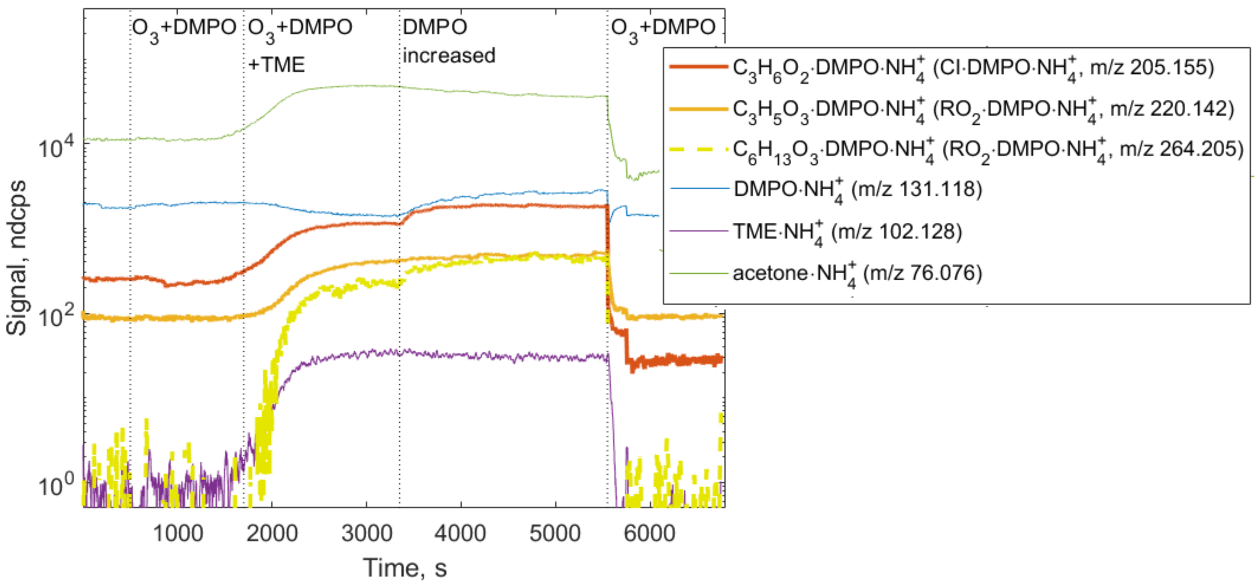

Figure 6: Ion tracers observed by NH_4^+ CIMS in a TME ozonolysis experiment as a function of different reactant conditions. Reactant concentrations are [TME] = 3.69×10^{11}; [O_3] = 7.87×10^{12}; [DMPO] = 2.01×10^{12} molecule cm^{-3}.

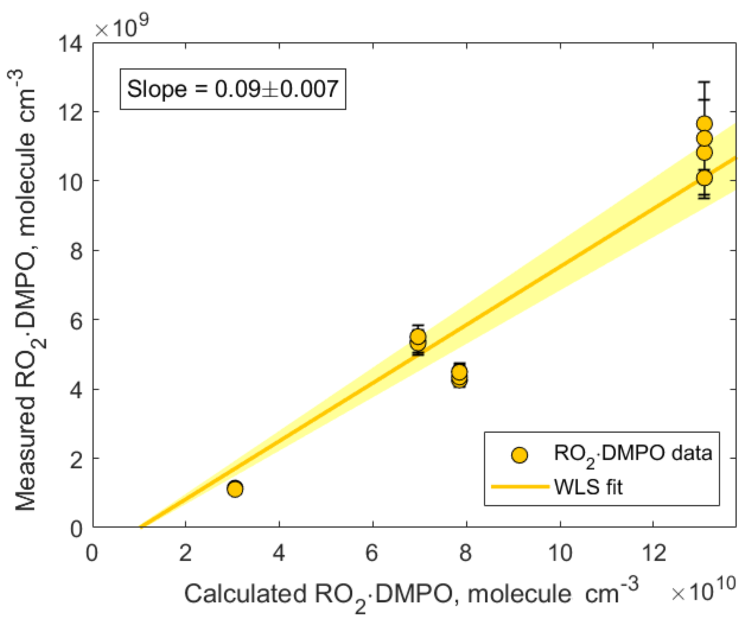

Figure 7: Correlation plot comparing measured and calculated concentrations of $CH_3C(=O)CH_2OO$·DMPO. The adducts were detected using NH_4^+ CIMS as $CH_3C(=O)CH_2OO$·DMPO·NH_4^+ (*m/z* 220.142). The slope is calculated using weighted least squares (WLS). A 95% confidence interval is estimated via a Monte Carlo simulation (N=5000) and shown using yellow shading.

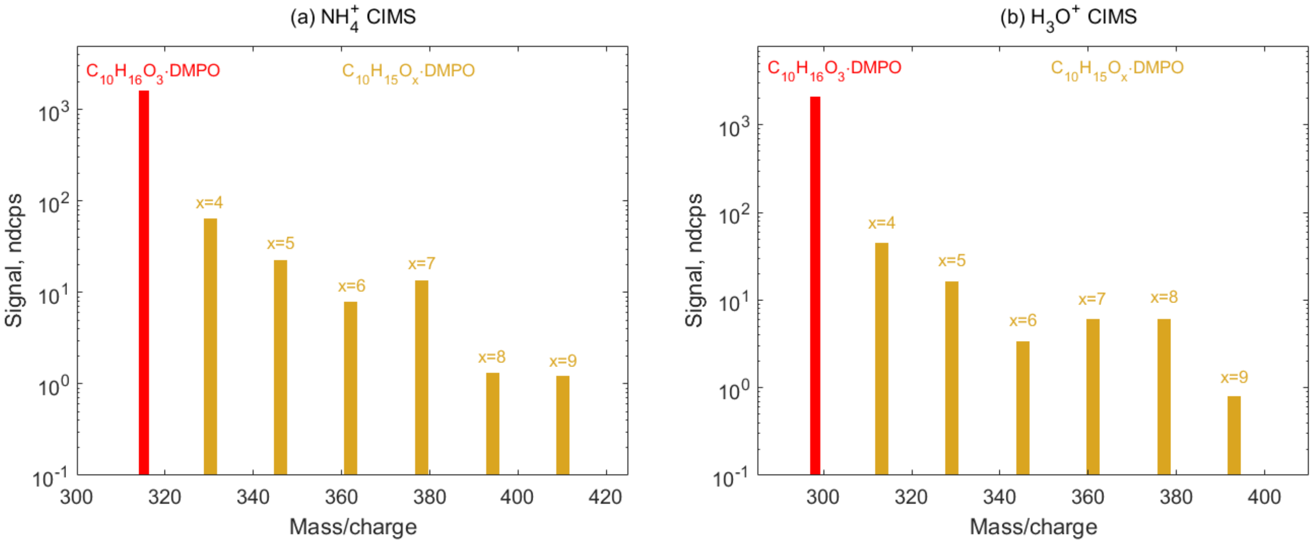

Figure 8: Mass spectra of SCI·DMPO (red) and RO_2·DMPO (yellow) adducts in α-pinene ozonolysis experiments observed using (a) NH_4^+ CIMS and (b) H_3O^+ CIMS. Primary RO_2 species ($C_{10}H_{15}O_4$) are formed via CI isomerization and can in turn undergo various autoxidation reactions resulting in formation of several organic peroxy radicals ($C_{10}H_{15}O_x$, x=5-9), which were detected bas adducts with the spin trap DMPO by the means of NH_4^+ and H_3O^+ CIMS.